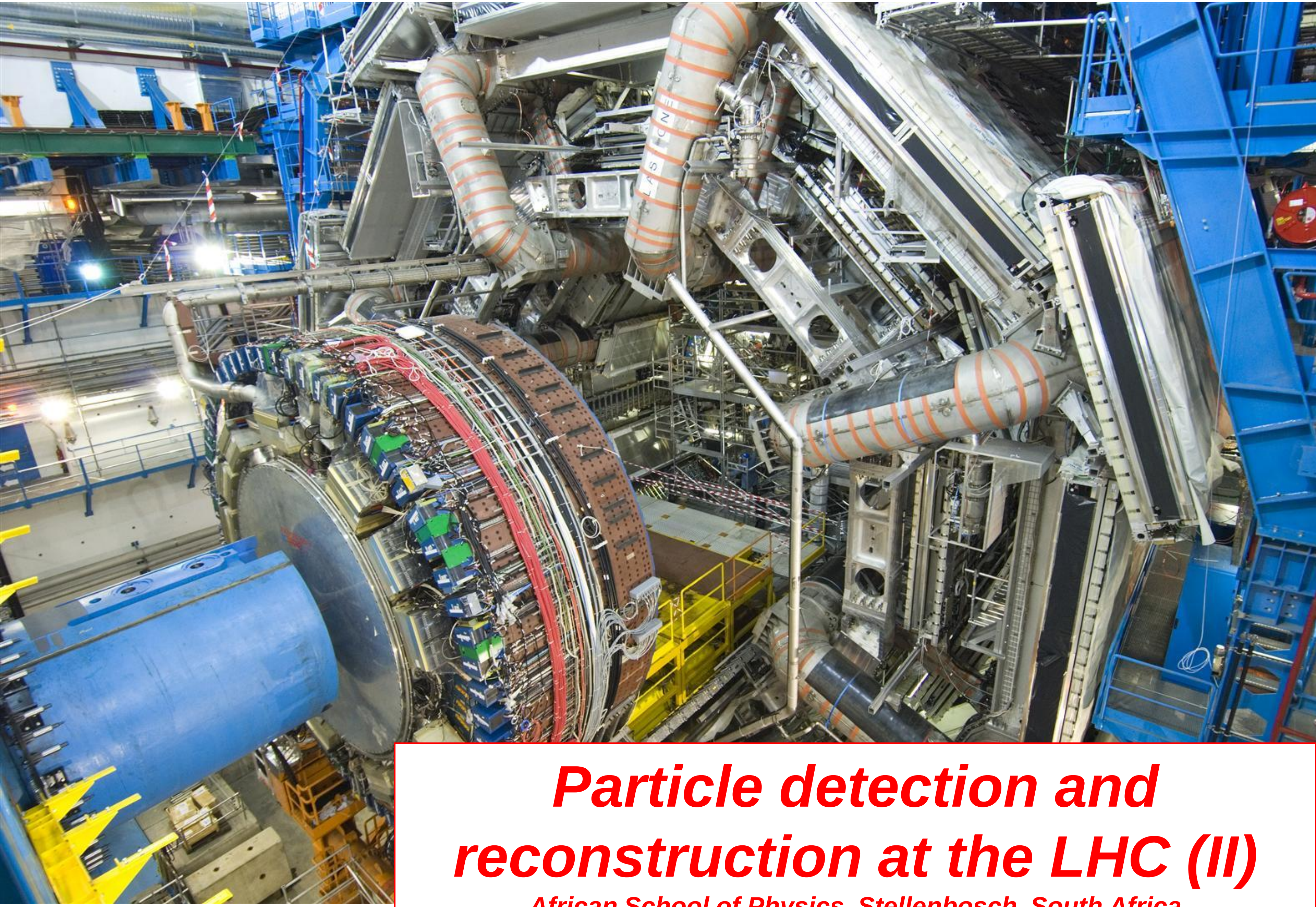

Particle detection and reconstruction at the LHC (II)

African School of Physics, Stellenbosch, South Africa
August 2010 (D. Froidevaux, CERN)

Particle detection and reconstruction at the LHC (and Tevatron)

Lecture 1

- Introduction to ATLAS/CMS experiments at the LHC
- Experimental environment and main design choices

Lecture 2

- Detector techniques: tracking

Lecture 3

- Detector techniques: calorimetry
- Detector techniques: trigger overview

The ATLAS Inner Detector (barrel)

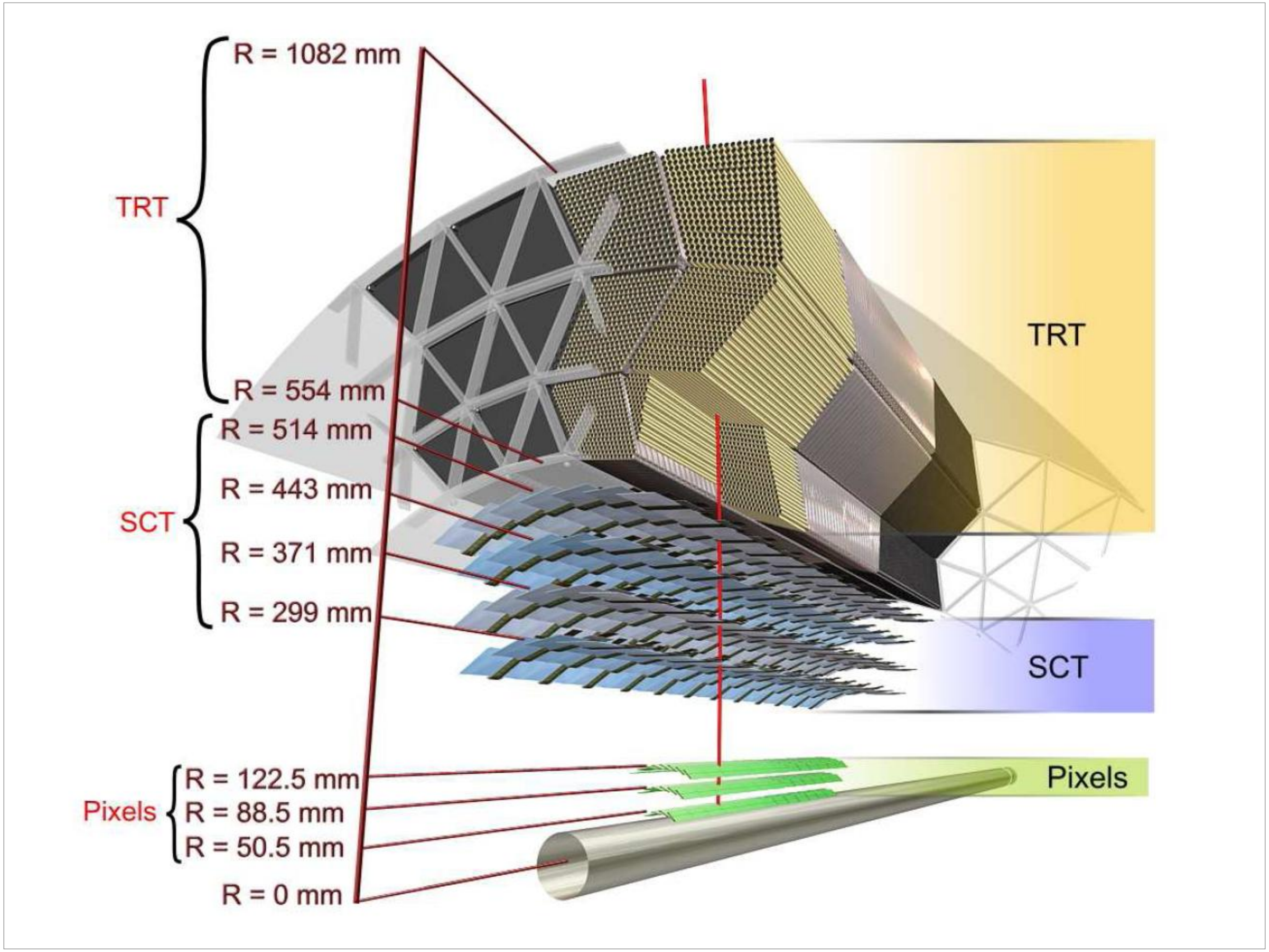

The ATLAS Inner Detector (one end-cap)

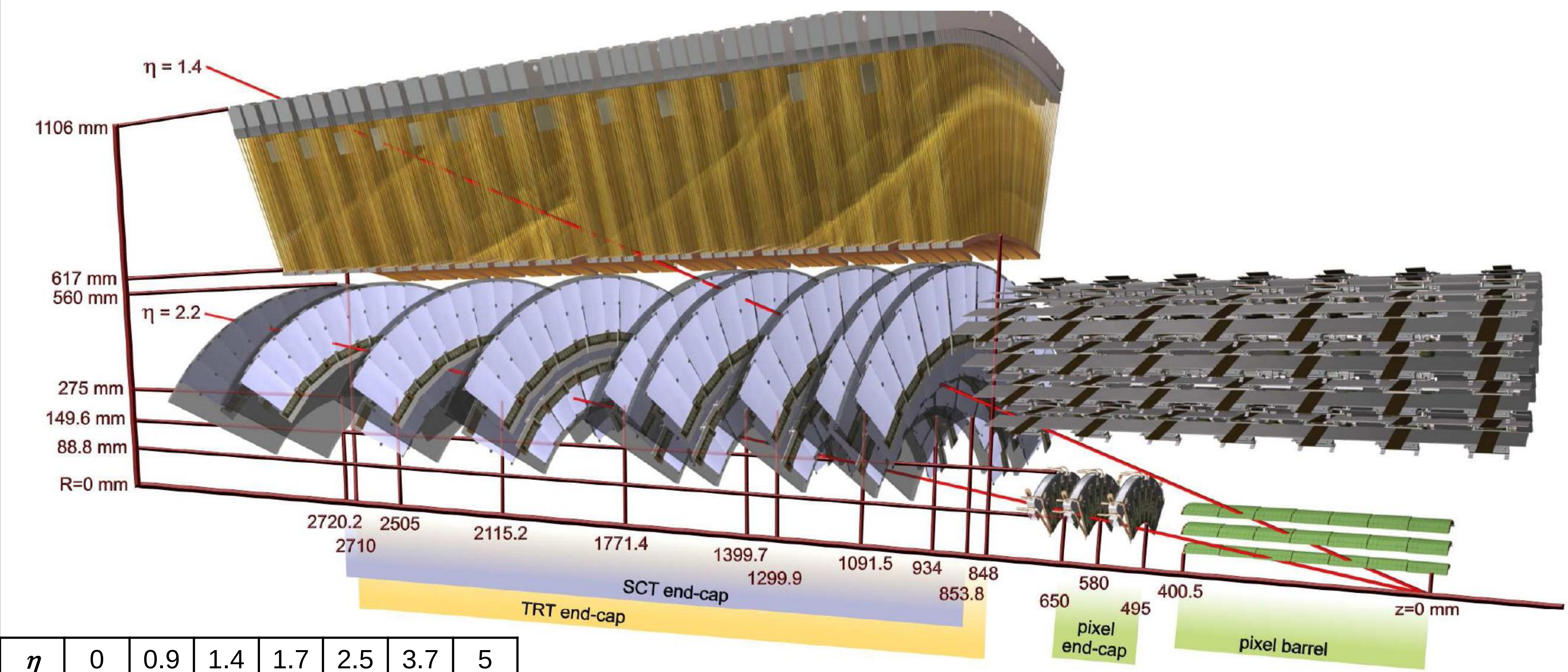

η	0	0.9	1.4	1.7	2.5	3.7	5
θ	90°	44°	28°	21°	9.4°	2.8°	0.8°

Electromagnetic Interaction of Particles with Matter

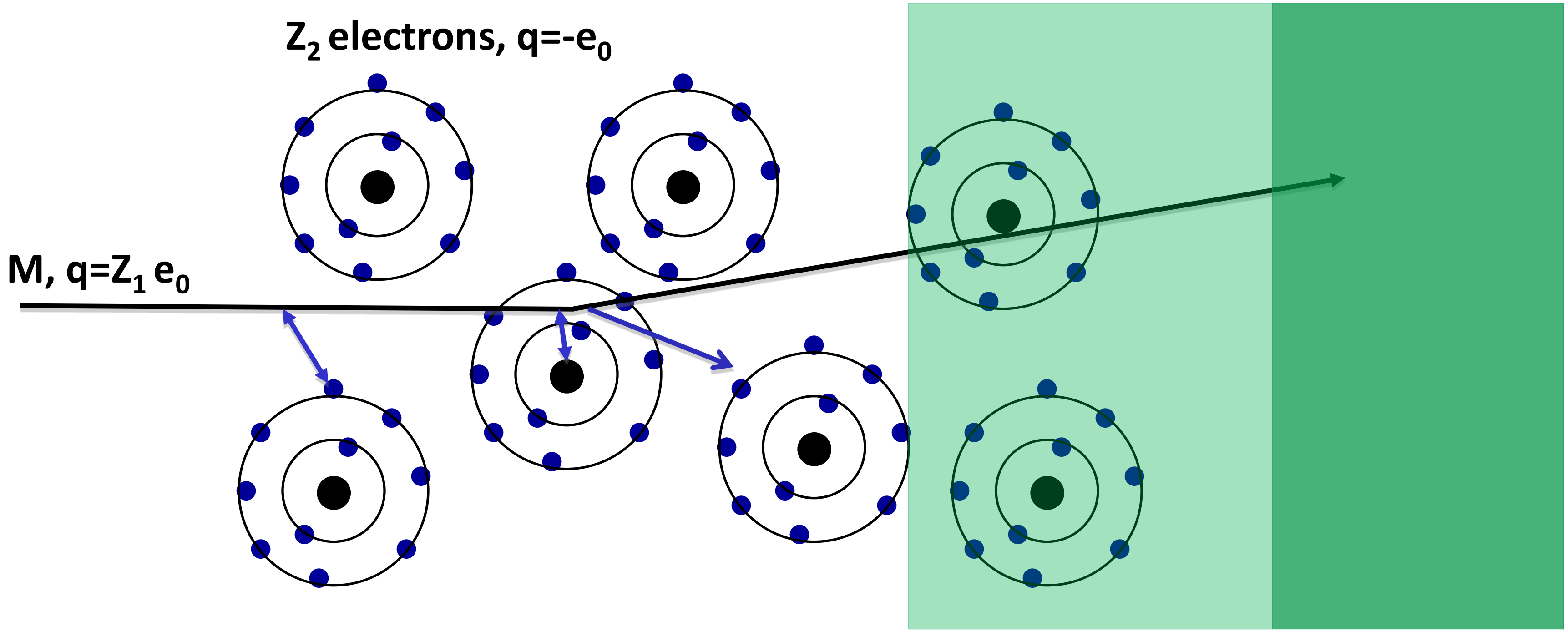

Interaction with the atomic electrons. The incoming particle loses energy and the atoms are excited or ionised.

Interaction with the atomic nucleus. The particle is deflected (scattered) causing Multiple Scattering of the particle in the material. During this scattering, Bremsstrahlung photons can be emitted.

In case the particle's velocity is larger than the velocity of light in the medium, the resulting EM shock-wave manifests itself as Cherenkov Radiation. When the particle crosses the boundary between two media, there is a probability of the order of 1% to produce X-ray photons, a phenomenon called Transition radiation.

Charged Particle Interactions with Matter

- Particles are detected through their interaction with the active detector materials

  - **Energy loss by ionisation**

Primary ionisation can generate secondary ionisation

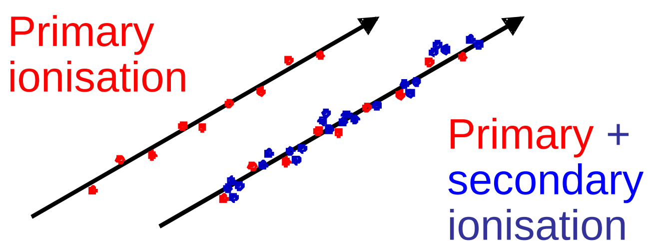

Typically:
Total ionisation = 3 x primary ionisation
→ ~ 90 electrons/cm in gas at 1 bar

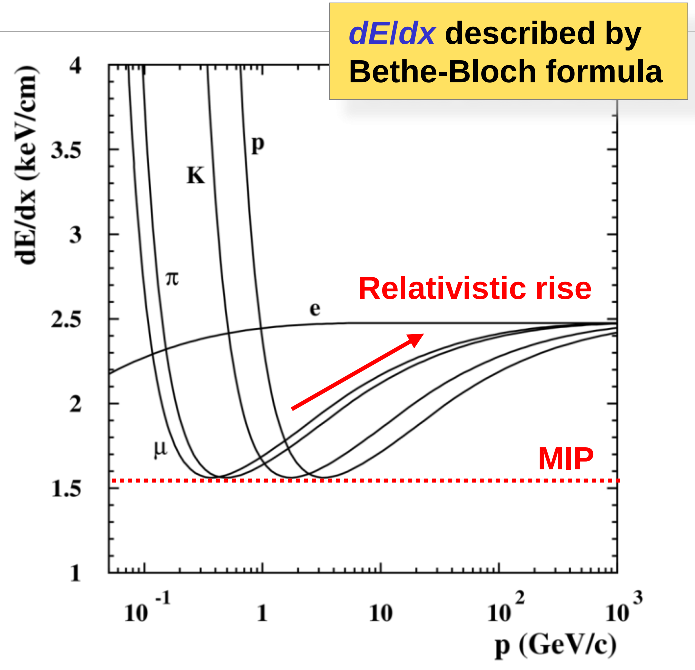

➡ Not directly used for PID by ATLAS/CMS

Charged Particle Interactions with Matter

- Particles are detected through their interaction with the active detector materials

  - Energy loss by ionisation
  - **Bremsstrahlung**

Due to interaction with Coulomb field of nucleus

Dominant energy loss mechanism for electrons down to low momenta (~10 MeV)

Initiates EM cascades (showers)

Charged Particle Interactions with Matter

- Particles are detected through their interaction with the active detector materials
  - Energy loss by ionisation
  - Bremsstrahlung
  - **Multiple scattering**

Challenges in Tracking

e^+ e^- collision in the ALEPH Experiment/LEP.

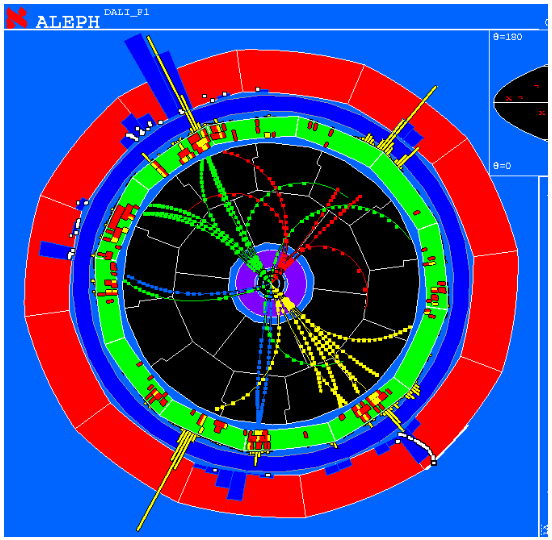

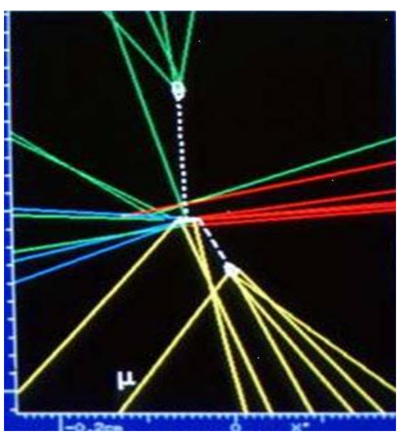

Au^+ Au^+ collision in the STAR Experiment/RHIC

Up to 2000 tracks

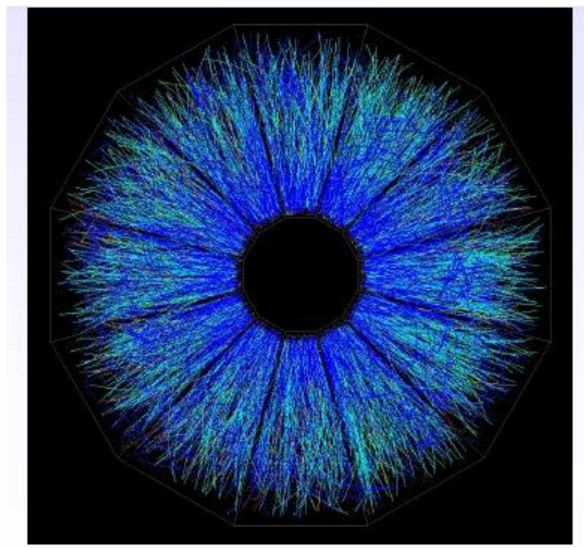

Pb+ Pb+ Collision in the ALICE Experiment/LHC

Simulation for

Angle ∪=60 to 62º

Up to 40 000 tracks/collision

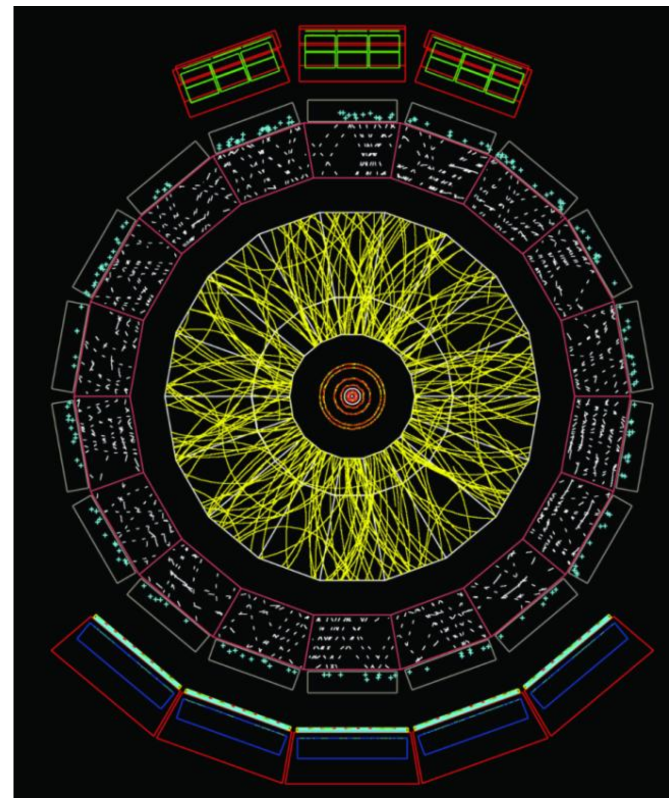

Energy Loss of Charged Particles by Atomic Collisions

A charged particle passing through matter suffers
1. energy loss
2. deflection from incident direction

Main type of reactions:
1. Inelastic collisions with atomic electrons of the material.
2. Elastic scattering from nuclei.

Less important reactions are:
3. Emission of Cherenkov radiation
4. Nuclear reactions
5. Bremsstrahlung (except for electrons!)

Classification of charged particles with respect to interactions with matter:
1. Low mass: electrons and positrons
2. High mass: muons, pions, protons, light nuclei.

Energy loss:
- mainly due to inelastic collisions with atomic electrons.
- cross section $\sigma \cong 10^{-17}$ - 10^{-16} cm^2 !
- small energy loss in each collision, but many collisions in dense material. Thus one can work with average energy loss.
- Example: a proton with E_{kin}=10 MeV loses all its energy after 0.25 mm of copper.

Two groups of inelastic atomic collisions:
- soft collisions: only excitation of atom.
- hard collisions: ionisation of atom. In some of the hard collisions the atomic electron get such a large energy that it causes secondary ionisation (δ-electrons).

Elastic collisions from nuclei cause very small energy loss. They are the main cause for deflection.

Bethe-Bloch Formula

Bethe-Bloch formula gives the mean rate of energy loss (stopping power) of a heavy charged particle.

$$-\frac{dE}{dx} = Kz^2 \frac{Z}{A} \frac{1}{\beta^2} \left[\frac{1}{2} \ln \frac{2m_e c^2 \beta^2 \gamma^2 T_{max}}{I^2} - \beta^2 - \frac{\delta(\beta\gamma)}{2} \right]$$

PDG 2008

with

A : atomic mass of absorber

$\frac{K}{A} = 4\pi N_A r_e^2 m_e c^2 / A = 0.307075 \text{ MeV g}^{-1}\text{cm}^2, \text{ for A} = 1\text{g mol}^{-1}$

z: atomic number of incident particle

Z: atomic number of absorber

T_{max} : Maximum energy transfer in a single collision $T_{max} = \frac{2m_e c^2 \beta^2 \gamma^2}{1 + 2\gamma m_e/M + (m_e/M)^2}$

δ(βγ) : density effect correction to ionisation loss.

x = ρ s , surface density or mass thickness, with unit g/cm^2, where s is the length.

dE/dx has the units MeV cm^2/g

History of Energy Loss Calculations: dE/dx

1915: Niels Bohr, classical formula, Nobel prize 1922.
1930: Non-relativistic formula found by Hans Bethe
1932: Relativistic formula by Hans Bethe

Bethe's calculation is leading order in pertubation theory, thus only z^2 terms are included.

Hans Bethe
1906-2005

Born in Strasbourg, emigrated to US in 1933.
Professor at Cornell U.
Nobel prize 1967
for theory of nuclear processes in stars.

Additional corrections:

- z^3 corrections calculated by Barkas-Andersen

- z^4 correction calculated by Felix Bloch (Nobel prize 1952, for nuclear magnetic resonance). Although the formula is called Bethe-Bloch formula the z^4 term is usually not included.

- Shell corrections: atomic electrons are not stationary

- Density corrections: by Enrico Fermi (Nobel prize 1938, for discovery of nuclear reaction induced by slow neutrons).

Examples of Mean Energy Loss

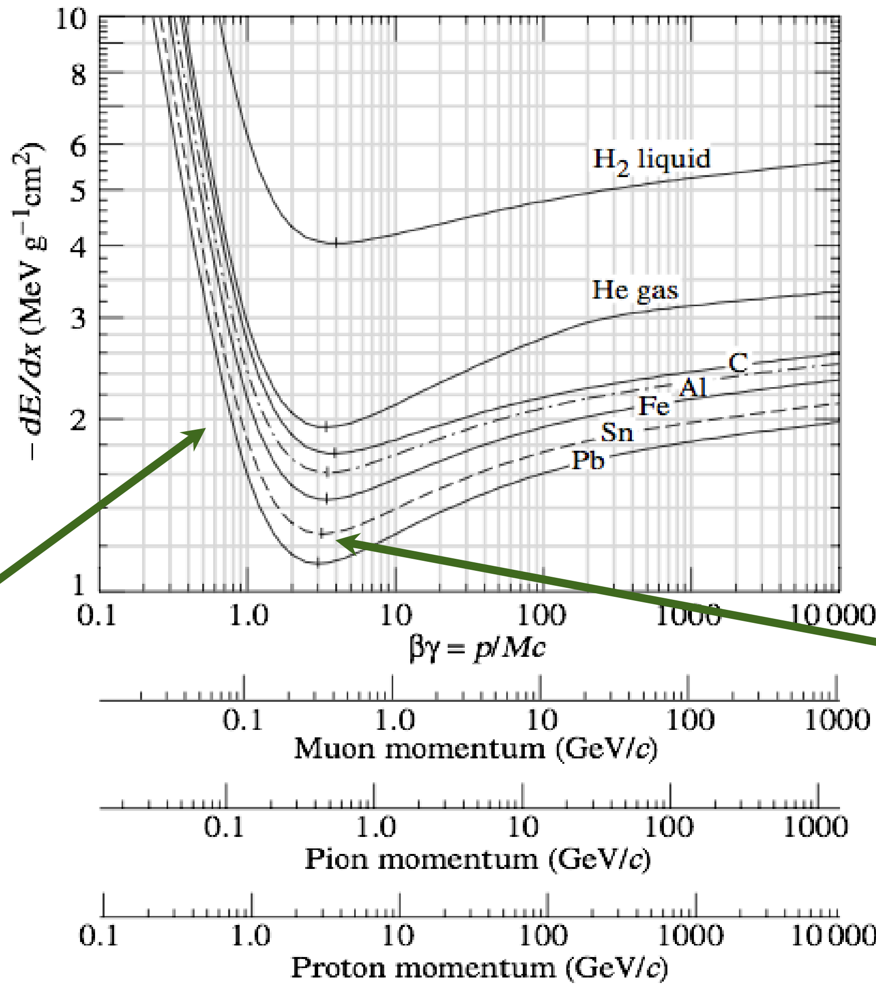

Figure 27.3: Mean energy loss rate in liquid (bubble chamber) hydrogen, gaseous helium, carbon, aluminum, iron, tin, and lead. Radiative effects, relevant for muons and pions, are not included. These become significant for muons in iron for $\beta\gamma \gtrsim 1000$, and at lower momenta for muons in higher-Z absorbers. See Fig. 27.21.

$1/\beta^2$

Bethe-Bloch formula:

$$-\frac{dE}{dx} = Kz^2 \frac{Z}{A} \frac{1}{\beta^2} [\frac{1}{2} \ln f(\beta) - \beta^2 - \frac{\delta(\beta\gamma)}{2}]$$

Except in hydrogen, particles of the same velocity have similar energy loss in different materials.

The minimum in ionisation occurs at βγ = 3.5 to 3.0, as Z goes from 7 to 100

PDG 2008

Particle identification from dE/dx and p measurements

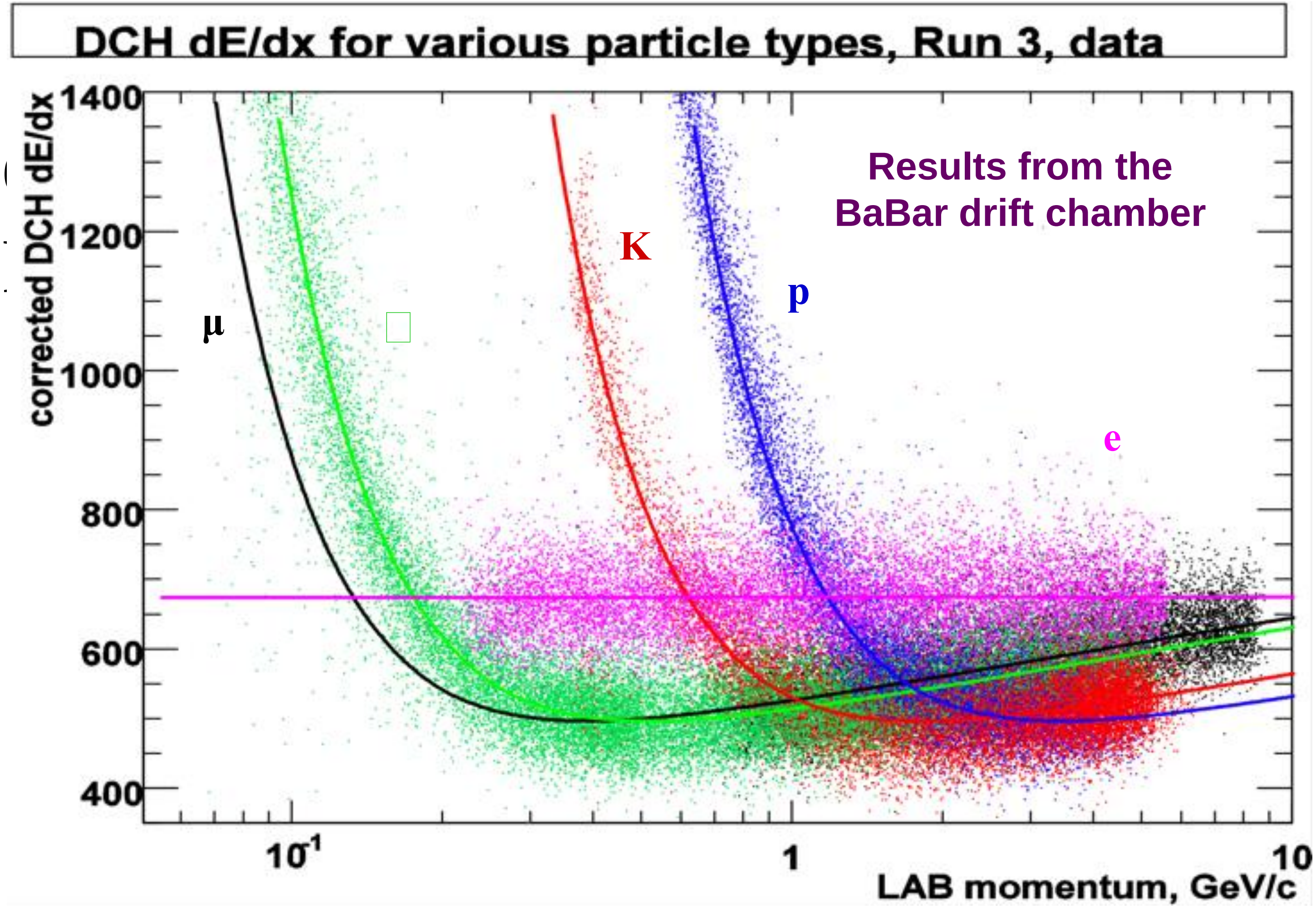

A simultaneous measurement of dE/dx and momentum can provide particle identification.

Bethe-Bloch Formula

Bethe Bloch Formula, a few numbers:

For Z ≈ 0.5 A
1/ρ dE/dx ≈ 1.4 MeV cm²/g for ßγ ≈ 3

Example :
Iron: Thickness = 100 cm; ρ = 7.87 g/cm³
dE ≈ 1.4 * 100* 7.87 = 1102 MeV

→ A 1 GeV Muon can traverse 1m of Iron

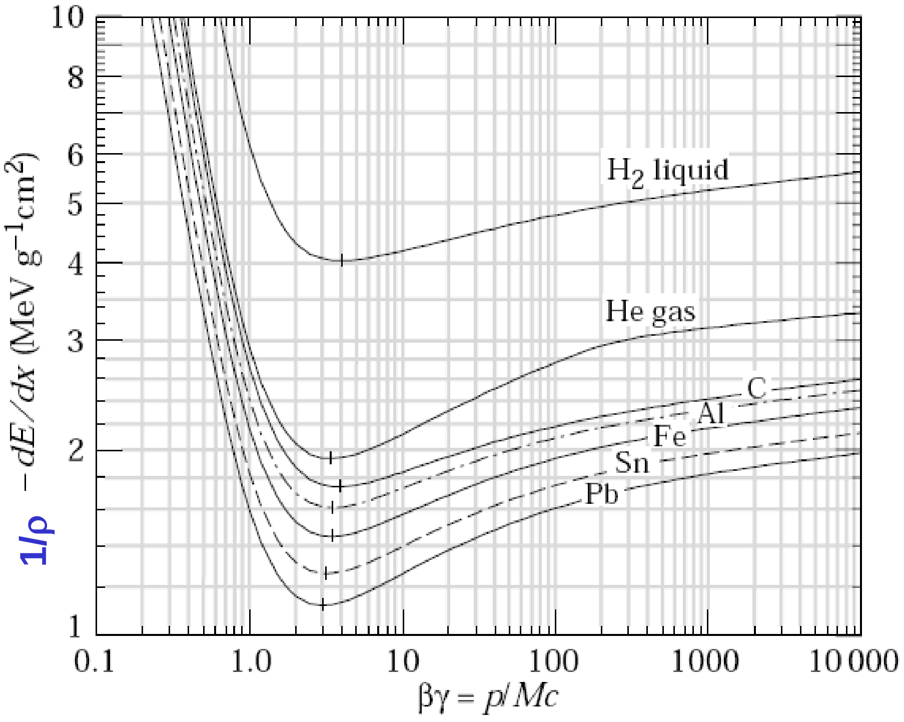

This number must be multiplied with ρ [g/cm³] of the material → dE/dx [MeV/cm]

Fluctuations in Energy Loss

Real detector (limited granularity) can not measure $<dE/dx>$!

It measures the energy ΔE deposited in a layer of finite thickness δx.

For thin layers or low density materials:

→ Few collisions, some with high energy transfer.

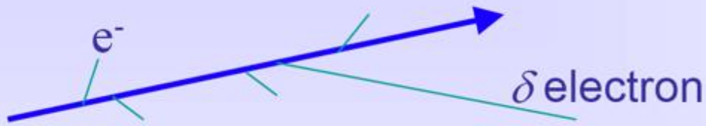

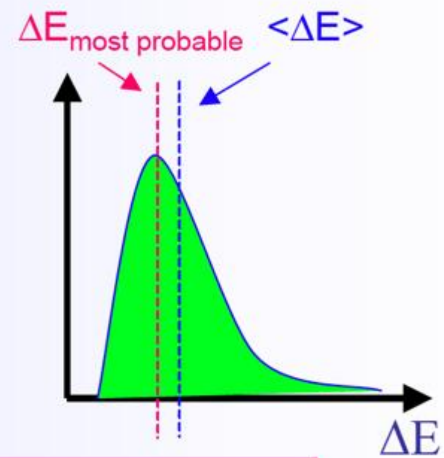

→ Energy loss distributions show large fluctuations towards high losses: "Landau tails"

Example: Si sensor: 300 μm thick. $\Delta E_{m.p} \sim 82$ keV $<\Delta E> \sim 115$ keV

For thick layers and high density materials:

→ Many collisions.

→ Central Limit Theorem → Gaussian shaped distributions.

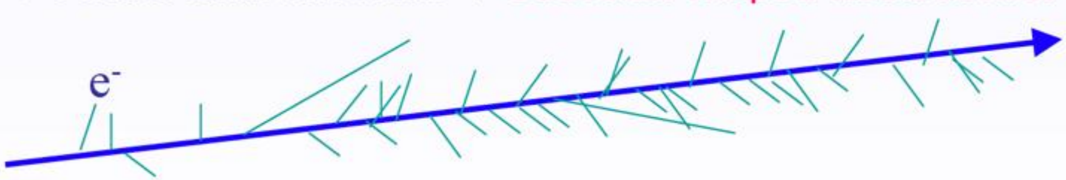

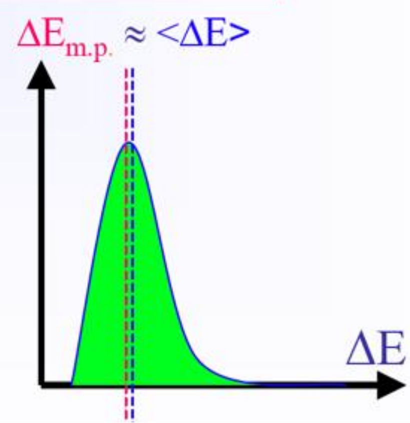

Range of Particles in Matter

Particle of mass M and kinetic Energy E_0 enters matter and looses energy until it comes to rest at distance R.

$$R(E_0) = \int_{E_0}^{0} \frac{-1}{dE/dx} dE$$

$$R(\beta_0\gamma_0) = \frac{Mc^2}{\rho} \frac{1}{Z_1^2} \frac{A}{Z} f(\beta_0\gamma_0)$$

$$\frac{\rho}{Mc^2} R(\beta_0\gamma_0) = \frac{1}{Z_1^2} \frac{A}{Z} f(\beta_0\gamma_0)$$

≈Independent of the material

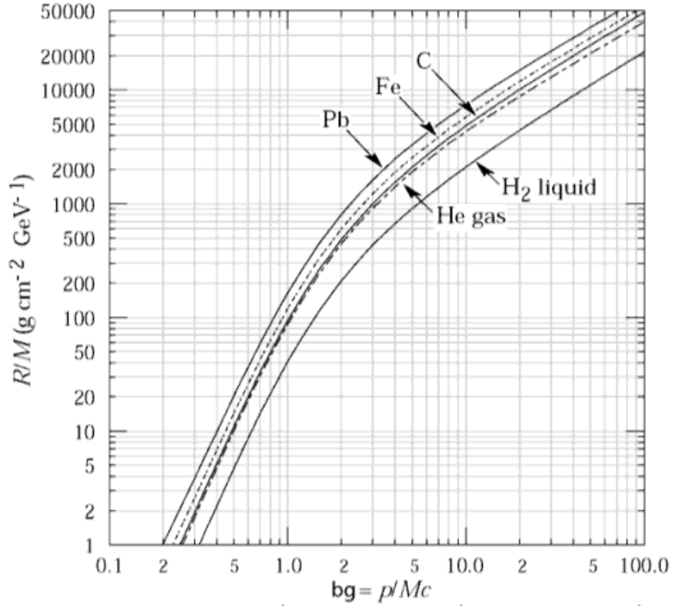

Bragg Peak:

For βγ>3 the energy loss is ≈ constant (Fermi Plateau)

If the energy of the particle falls below βγ=3 the energy loss rises as $1/\beta^2$

Towards the end of the track the energy loss is largest → Cancer Therapy.

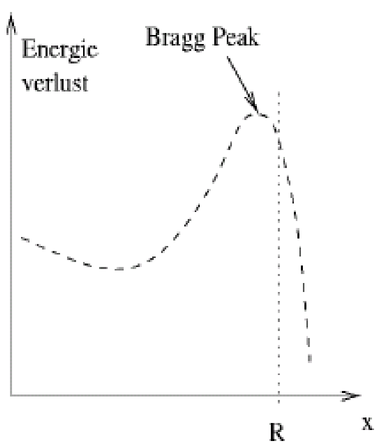

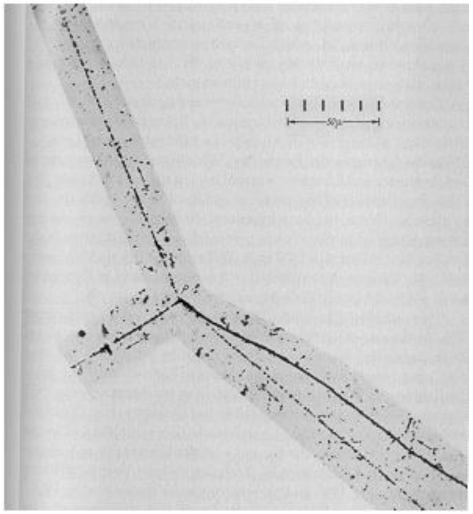

Range of Particles in Matter

Average Range:

Towards the end of the track the energy loss is largest → Bragg Peak → Cancer Therapy … or Archaeology!

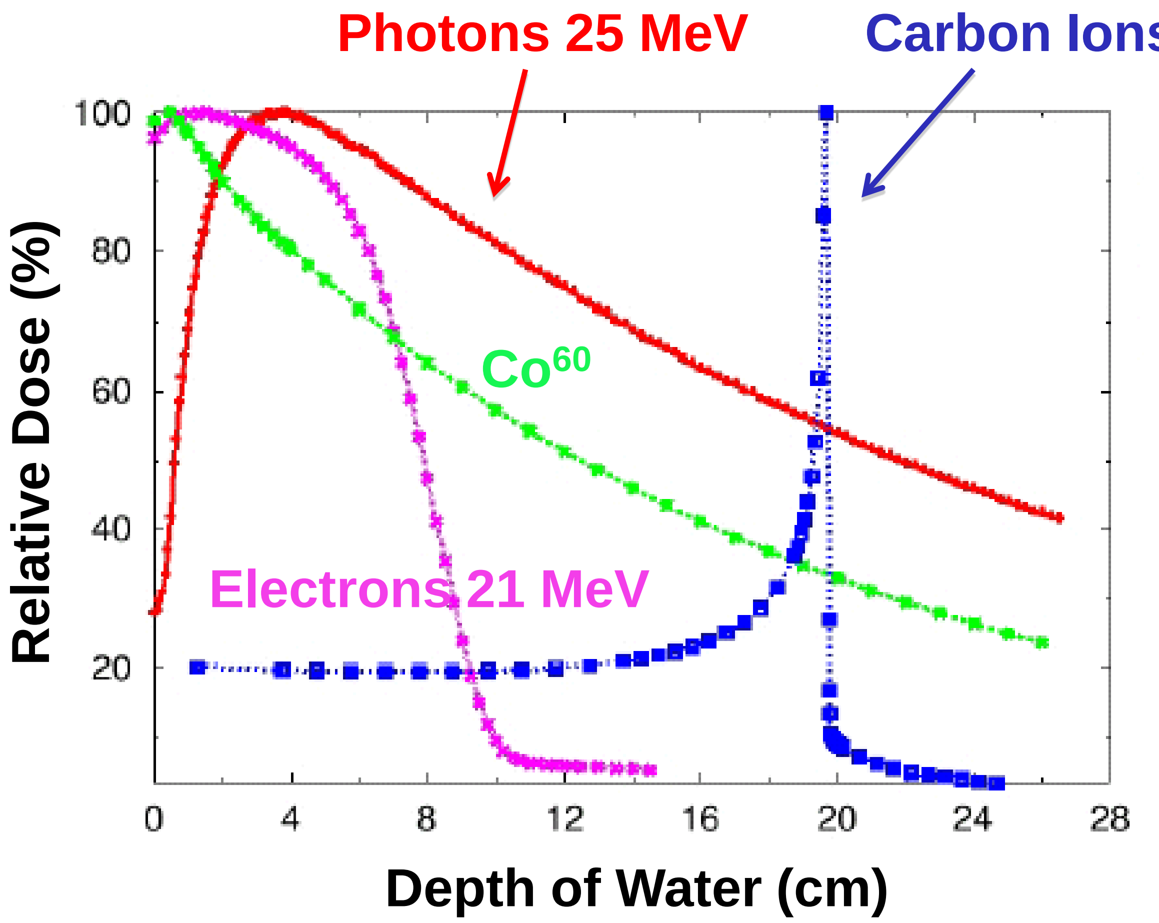

Search for Hidden Chambers in the Pyramids

The structure of the Second Pyramid of Giza is determined by cosmic-ray absorption.

Luis W. Alvarez, Jared A. Anderson, F. El Bedwei, James Burkhard, Ahmed Fakhry, Adib Girgis, Amr Goneid, Fikhry Hassan, Dennis Iverson, Gerald Lynch, Zenab Miligy, Ali Hilmy Moussa, Mohammed-Sharkawi, Lauren Yazolino

Fig. 2 (bottom right). Cross sections of (a) the Great Pyramid of Cheops and (b) the Pyramid of Chephren, showing the known chambers: (A) Smooth limestone cap, (B) the Belzoni Chamber, (C) Belzoni's entrance, (D) Howard-Vyse's entrance, (E) descending passageway, (F) ascending passageway, (G) underground chamber, (H) Grand Gallery, (I) King's Chamber, (J) Queen's Chamber, (K) center line of the pyramid.

6 FEBRUARY 1970

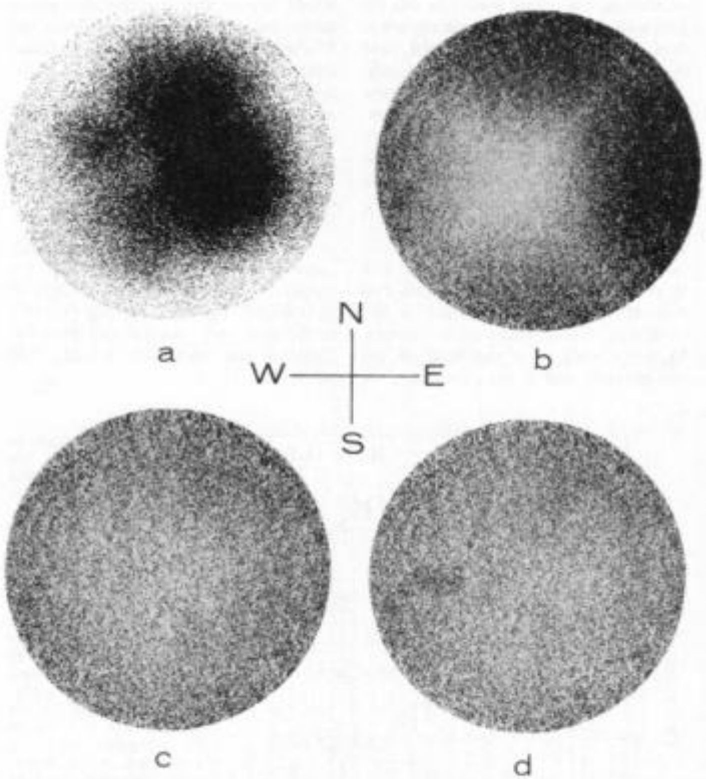

Fig. 13. Scatter plots showing the three stages in the combined analytic and visual analysis of the data and a plot with a simulated chamber. (a) Simulated "x-ray photograph" of uncorrected data. (b) Data corrected for the geometrical acceptance of the apparatus. (c) Data corrected for pyramid structure as well as geometrical acceptance. (d) Same as (c) but with simulated chamber, as in Fig. 12.

Luis Alvarez used the attenuation of muons to look for chambers in the Second Giza Pyramid

→

Muon Tomography

He proved that there are no chambers present.

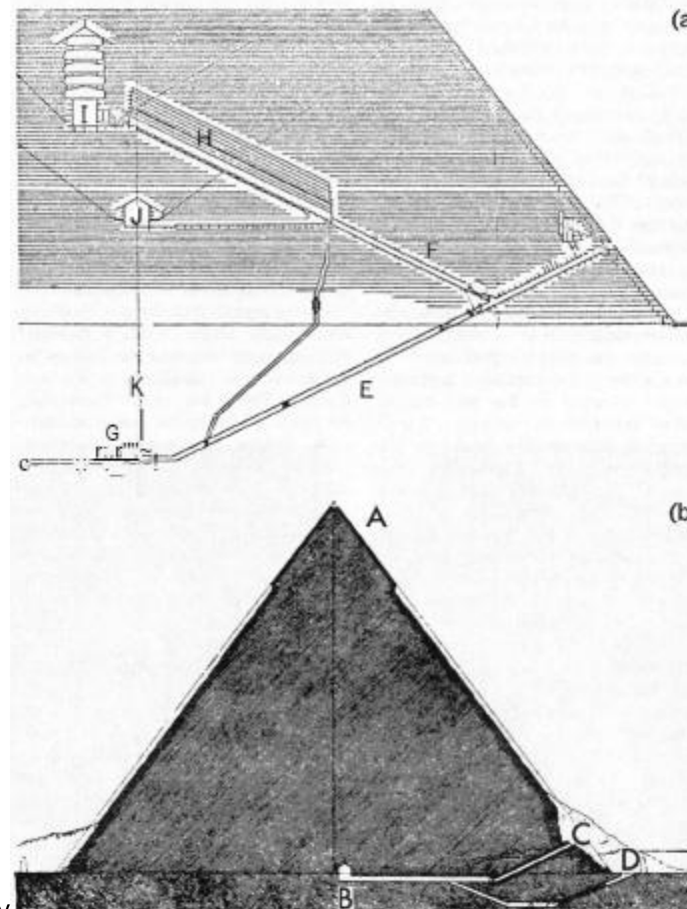

Multiple Coulomb Scattering

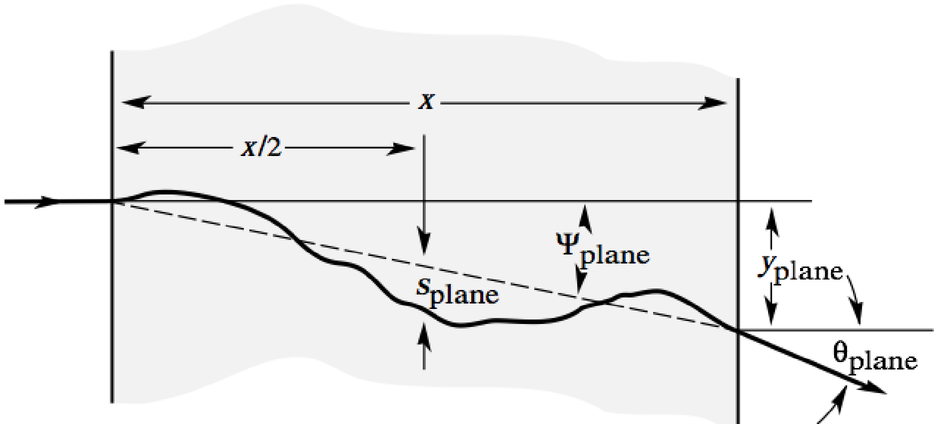

Figure 27.9: Quantities used to describe multiple Coulomb scattering. The particle is incident in the plane of the figure.

$$\psi^{\rm rms}_{\rm plane} = \frac{1}{\sqrt{3}}\,\theta^{\rm rms}_{\rm plane} = \frac{1}{\sqrt{3}}\,\theta_0 \; ,$$

$$y^{\rm rms}_{\rm plane} = \frac{1}{\sqrt{3}}\,x\,\theta^{\rm rms}_{\rm plane} = \frac{1}{\sqrt{3}}\,x\,\theta_0 \; ,$$

$$s^{\rm rms}_{\rm plane} = \frac{1}{4\sqrt{3}}\,x\,\theta^{\rm rms}_{\rm plane} = \frac{1}{4\sqrt{3}}\,x\,\theta_0 \; .$$

A particle which traverses a medium is deflected by small angle Coulomb scattering from nuclei. For hadronic particles also the strong interaction contributes.

The angular deflection after traversing a distance x is described by the Molière theory. The angle has roughly a Gauss distribution, but with larger tails due to Coulomb scattering.

Defining: $\theta_0 = \theta^{\rm rms}_{\rm plane} = \frac{1}{\sqrt{2}}\,\theta^{\rm rms}_{\rm space}$

Gaussian approximation:

$$\theta_0 = \frac{13.6\ {\rm MeV}}{\beta c p}\, z\, \sqrt{x/X_0}\Big[1 + 0.038 \ln(x/X_0)\Big]$$

x/X_0 is the thickness of the material in radiation lengths.

Bremsstrahlung

High energy electrons lose their energy predominantly through radiation (bremsstrahlung).

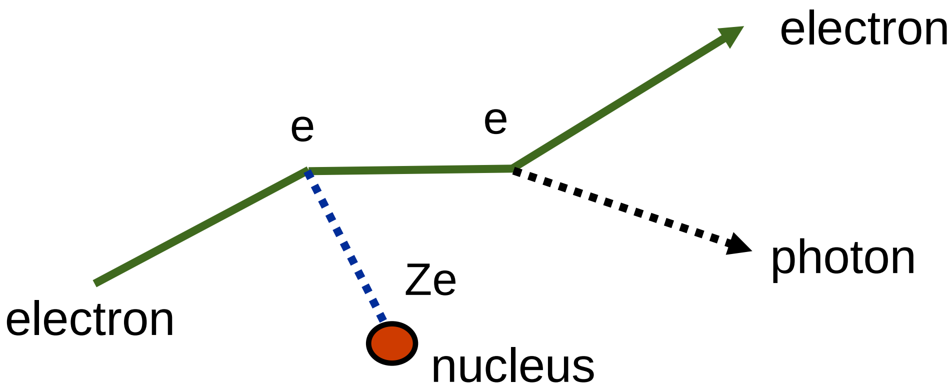

Cross section:

$\sigma \sim (Z\ e^3)^2 \sim Z^2\ \ \alpha^3$

The electron is decelerated (accelerated) in the field of the nucleus. Accelerated charges radiate photons. Thus the bremsstrahlung is strong for light charged particles (electrons), because its acceleration is large for a given force. For heavier particles like muons, bremsstrahlung effects are only important at energies of a few hundred GeV (important for ATLAS/CMS at the LHC!).

The presence of a nucleus is required to restore energy-momentum conservation. Thus the cross-section is proportional to Z^2 and α^3 (α = fine structure constant).

The characteristic length which an electron travels in material until a bremsstrahlung happens is the radiation length X_0.

Charged Particle Interactions with Matter

- Particles are detected through their interaction with the active detector materials

Inne Weight: 4.5 tons ough planning anc Weight: 3.7 tons

- Energy lo … sstrahlung
- Mult

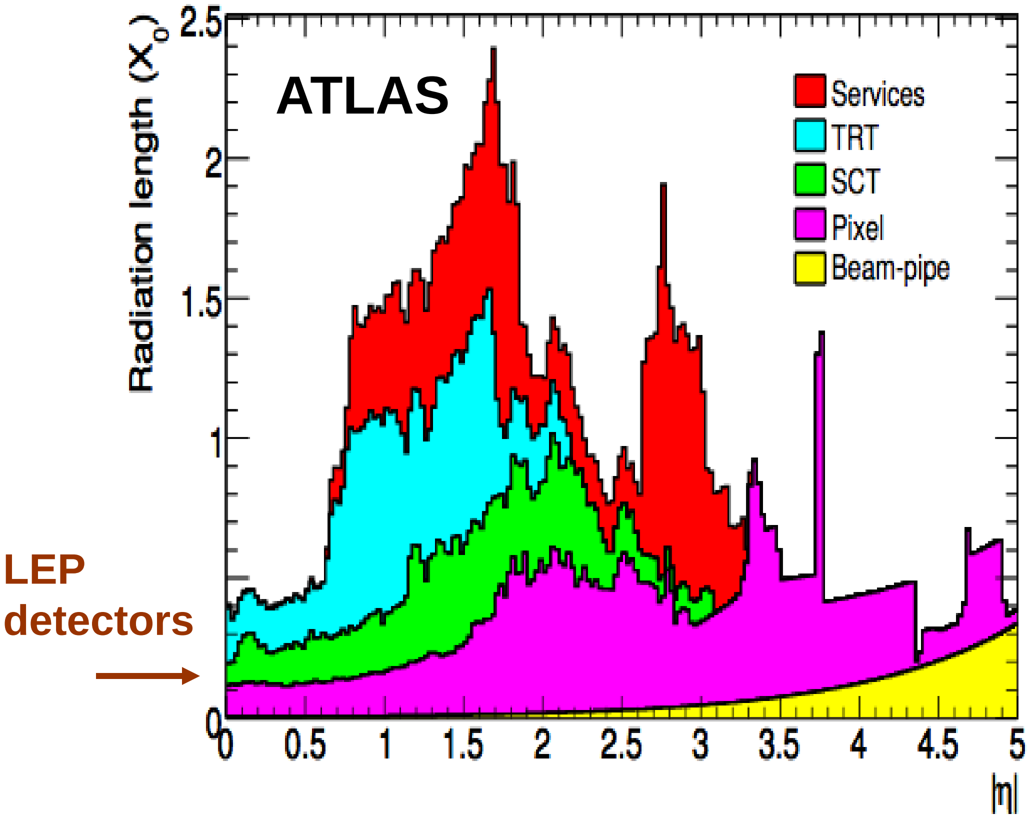

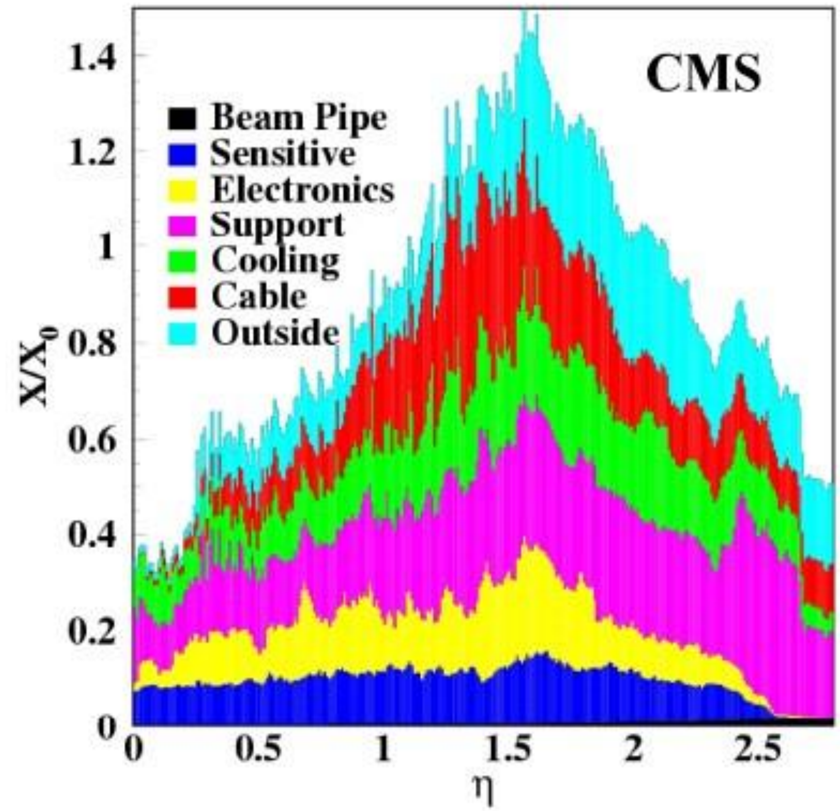

For ATLAS, need to add ~2 X_0 (η = 0) from solenoid + cryostat in front of EM calorimeter

Charged Particle Interactions with Matter

- Particles are detected through their interaction with the active detector materials
  - Energy loss by ionisation
  - Bremsstrahlung
  - Multiple scattering
  - Radiation length
  - **Cherenkov radiation**

A relativistic charge particle traversing a dielectric medium with refraction index $n > 1/\beta$, emits Cherenkov radiation in cone with angle θ_C around track: $\cos\theta_C = (n\beta)^{-1}$

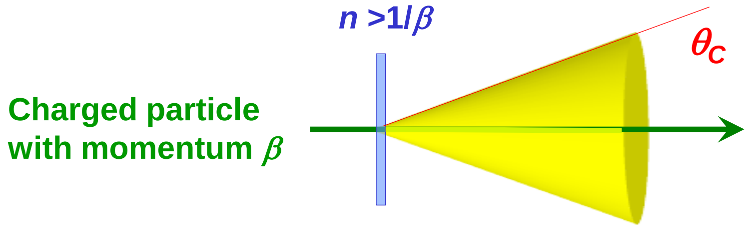

Light cone emission when passing thin medium

Detector types RICH (LHCb), DIRC, Aerogel counters (not employed by ATLAS/CMS))

Charged Particle Interactions with Matter

- Particles are detected through their interaction with the active detector materials
  - Energy loss by ionisation
  - Bremsstrahlung
  - Multiple scattering
  - Radiation length
  - Cherenkov radiation
  - **Transition radiation**

Photon radiation when charged ultra-relativistic particles traverse the boundary of two different dielectric media (foil & air)

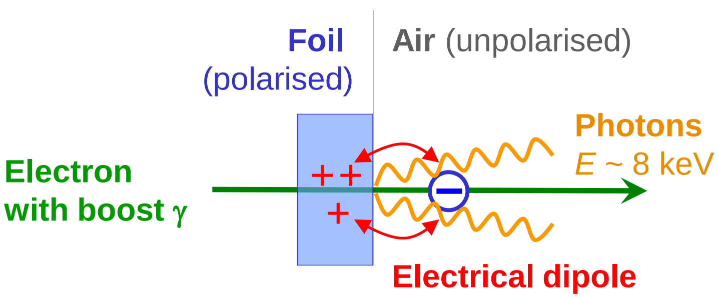

➡ Significant radiation for γ > 1000 and > 100 boundaries

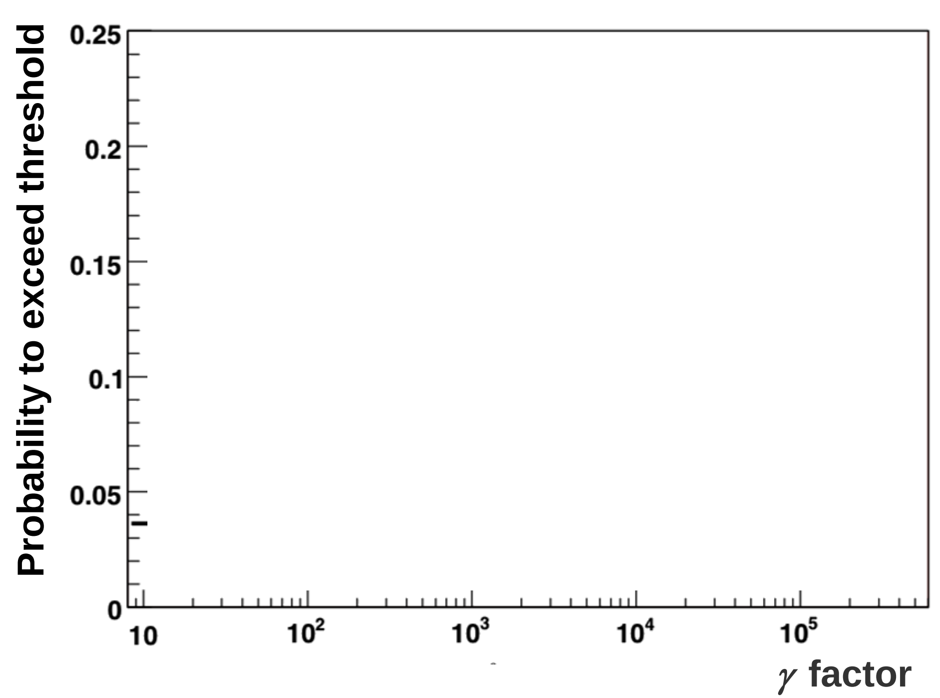

Semiconductor Trackers

Semiconductors

- Doping of silicon crystal semiconductors:

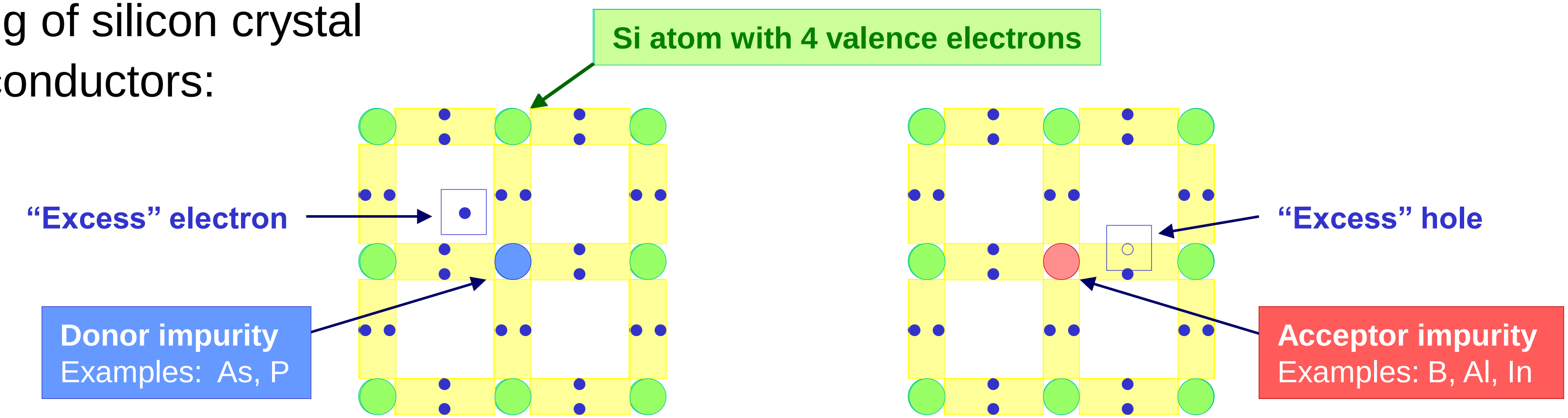

Reverse bias *p*–*n* junction

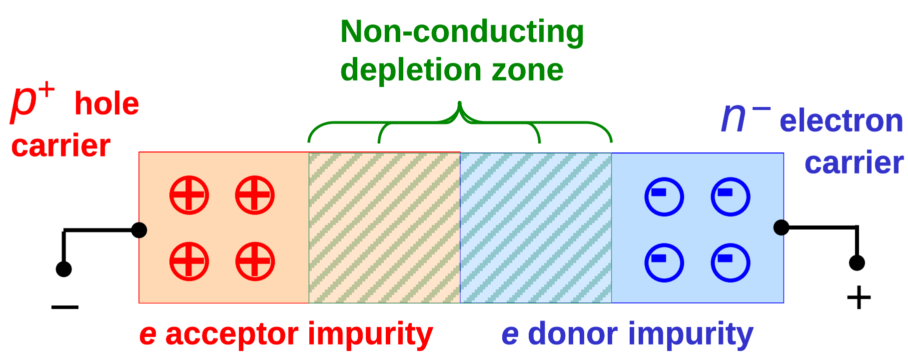

- The reverse bias voltage increases the potential barrier in the depletion zone, enhancing its resistance
- *n* doping adds electro-phobe atoms
- The potential barrier in the junction
- Minimal weight ... counter ... the doping ... potential

The *p–n* Junction as a Tracking Detector

- Thin (~μm), highly doped p^+ (~10^{19} cm^{-3}) layer on lightly doped *n* (~10^{12} cm^{-3}) substrate
  - High mobility of charge carriers in Si allows fast charge collection (~5 ns for electron)
  - High Si density & low electron–hole creation potential (3.6 eV compared to ~ 11-30 eV for gaseous ionisation) allows use of very thin detectors with reasonable signal

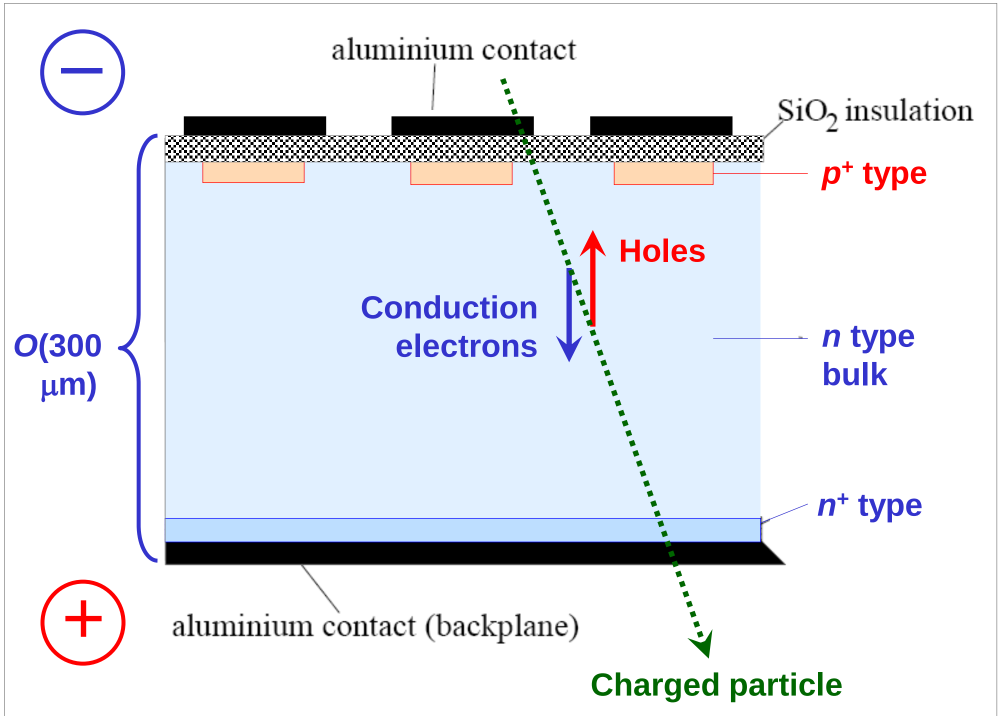

Schema of silicon microstrip sensor

- Reverse bias: backplane set to positive voltage (< 500 V)
- A traversing charged particle ionises silicon, creating conduction electrons and holes that induce a measurable current by drifting to electrodes
- Metal-semiconductor transition forms charge (Schottky) barrier similar to *p–n* junction. Highly doped n^+ layer reduces width of potential barrier and hence resistance

The ATLAS Semiconductor Tracker (SCT)

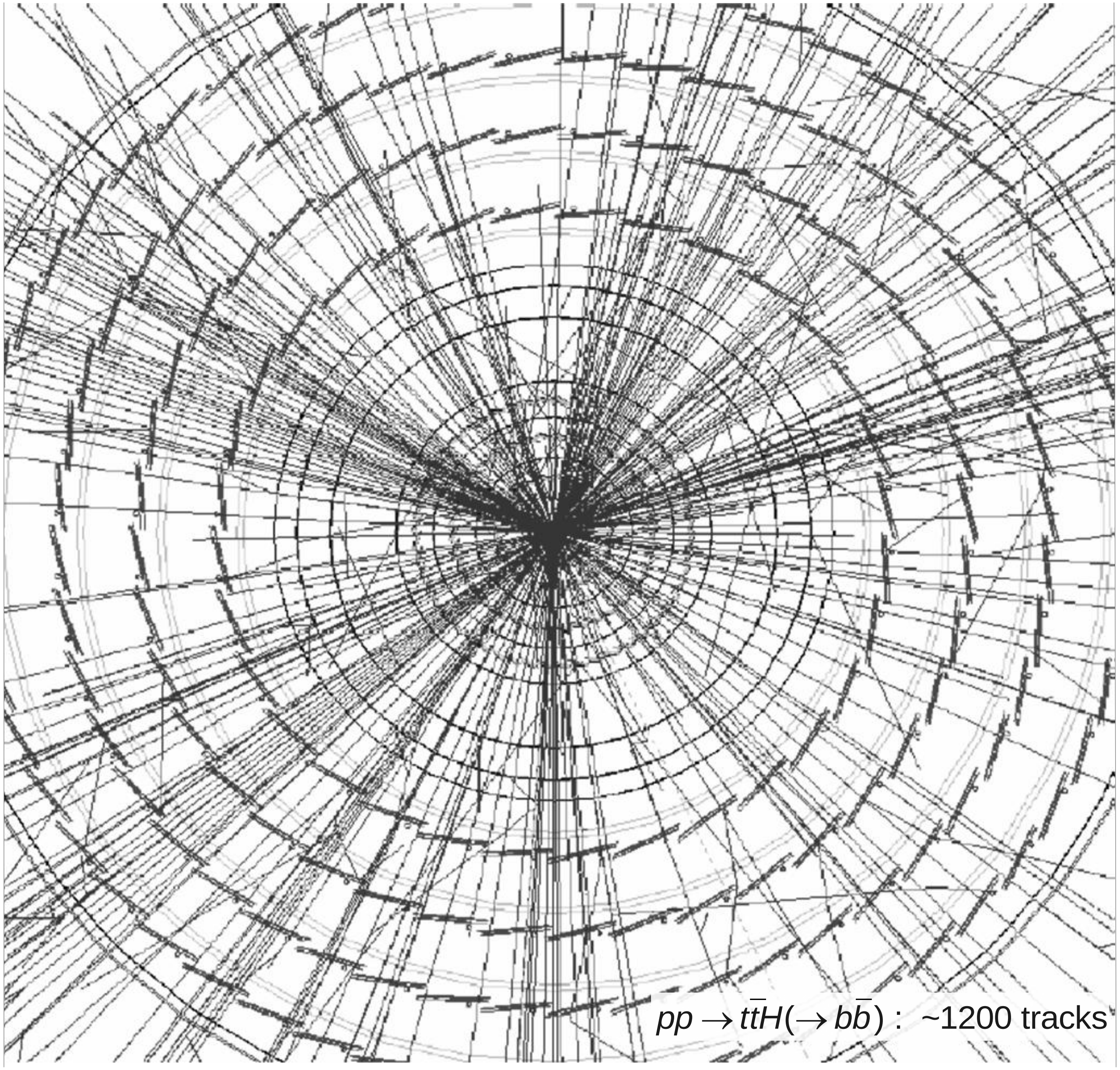

SCT Module

- Barrel SCT module:

Binary readout is mu
analog one (no ADC
cannot correct for co

Hybrid assembly
with readout chips

4 Silicon sensors
280 μm thick
2.3° stereo angle
Overlap in ϕ & z to adjacent modules

Be module baseboard with mounting points & central TPG

TPG (thermal pyrolythic graphite) plate for sensor cooling

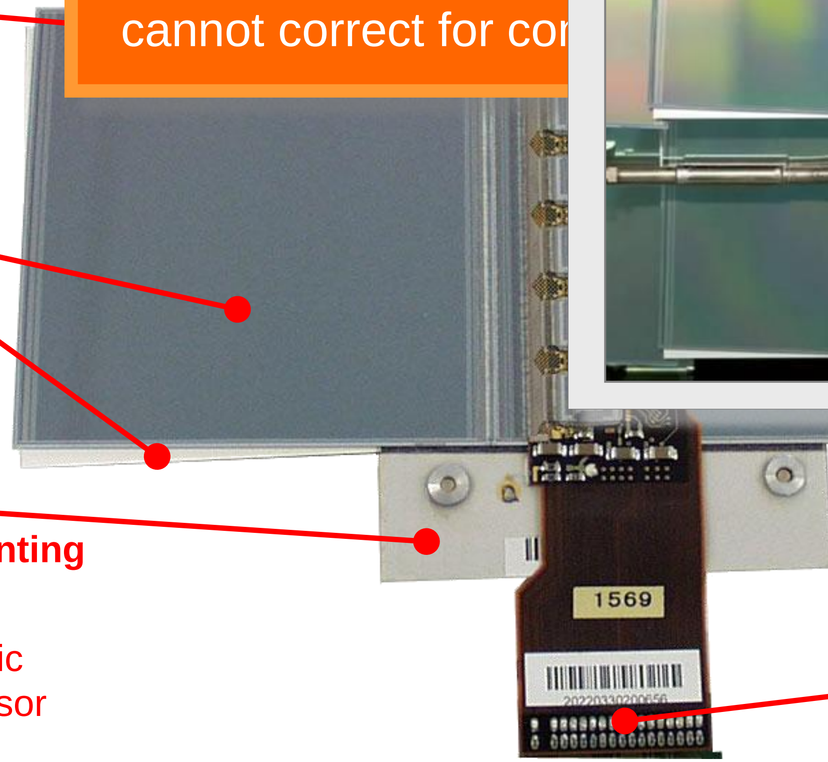

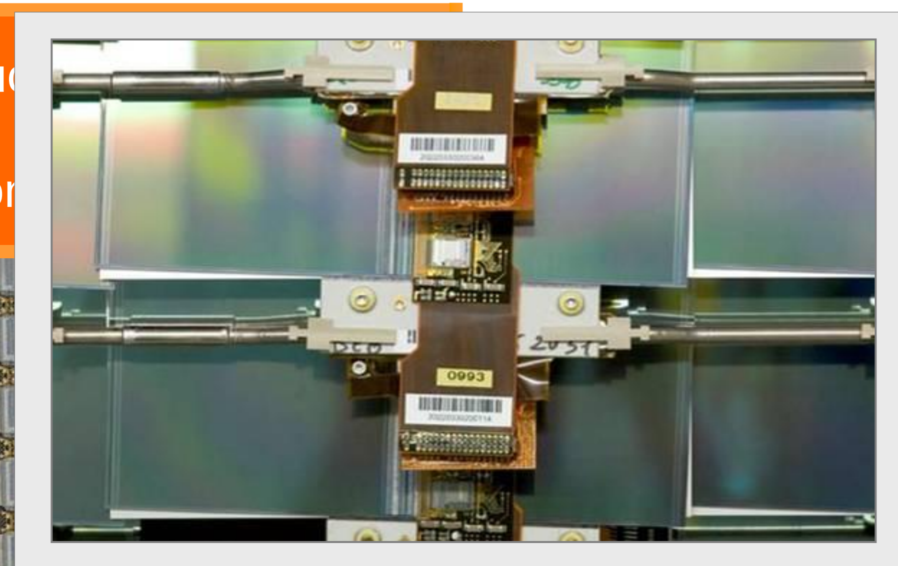

Connector
Power & data

Fully equipped double sided electrical module with baseboard and readout hybrids

Geometry of ATLAS SCT

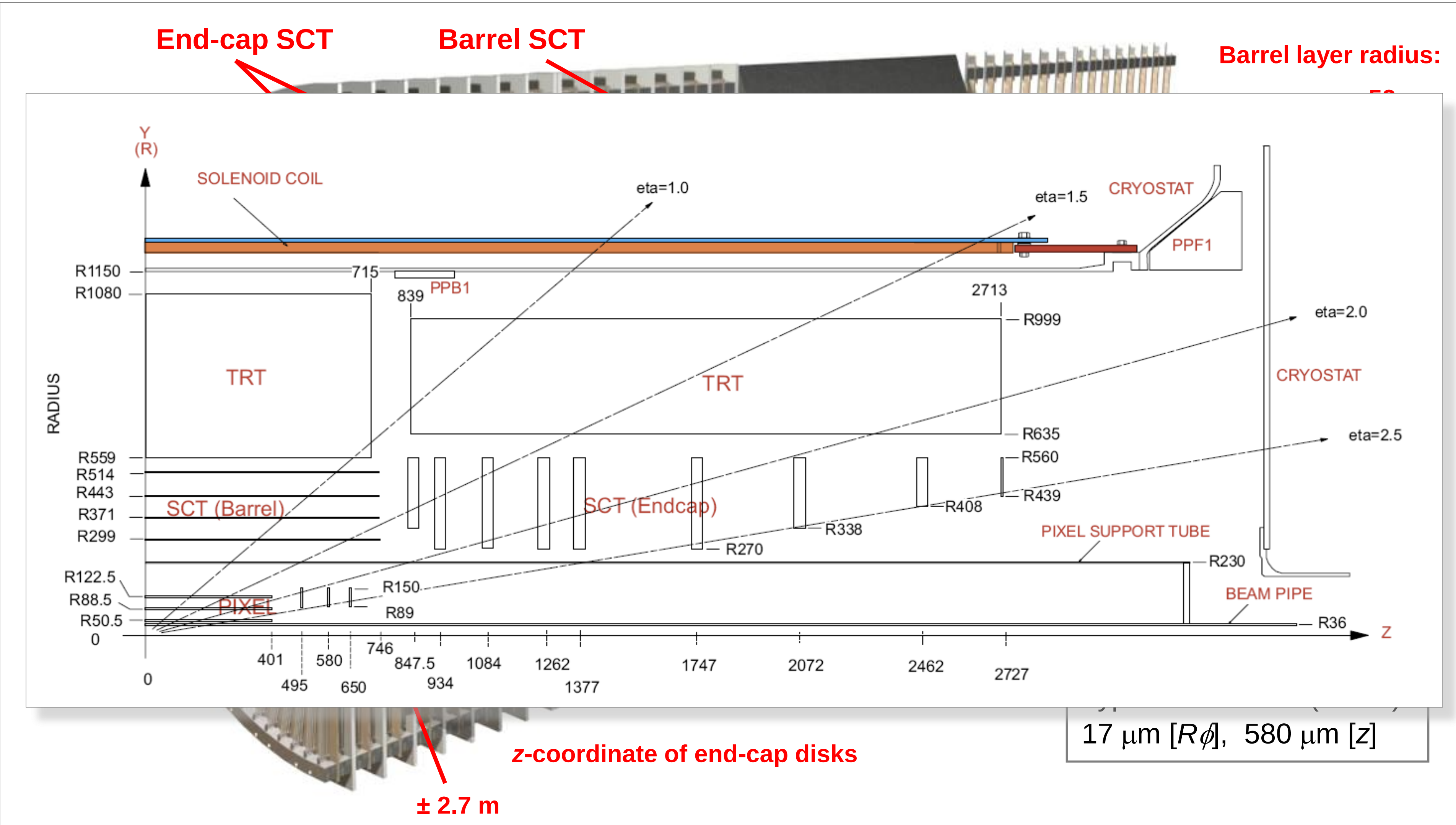

The ATLAS Semiconductor Tracker (SCT)

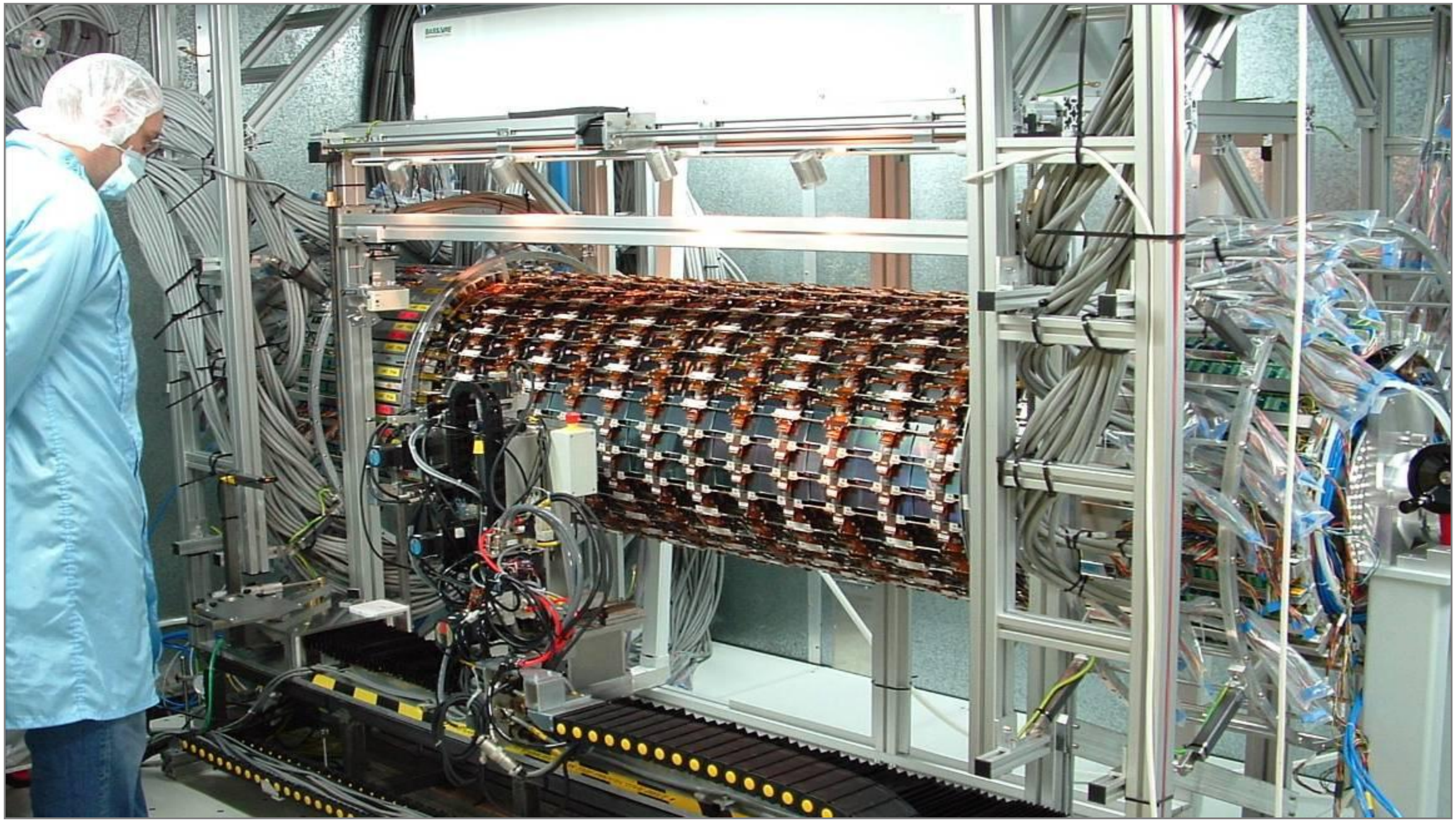

Lorentz Angle Measurement

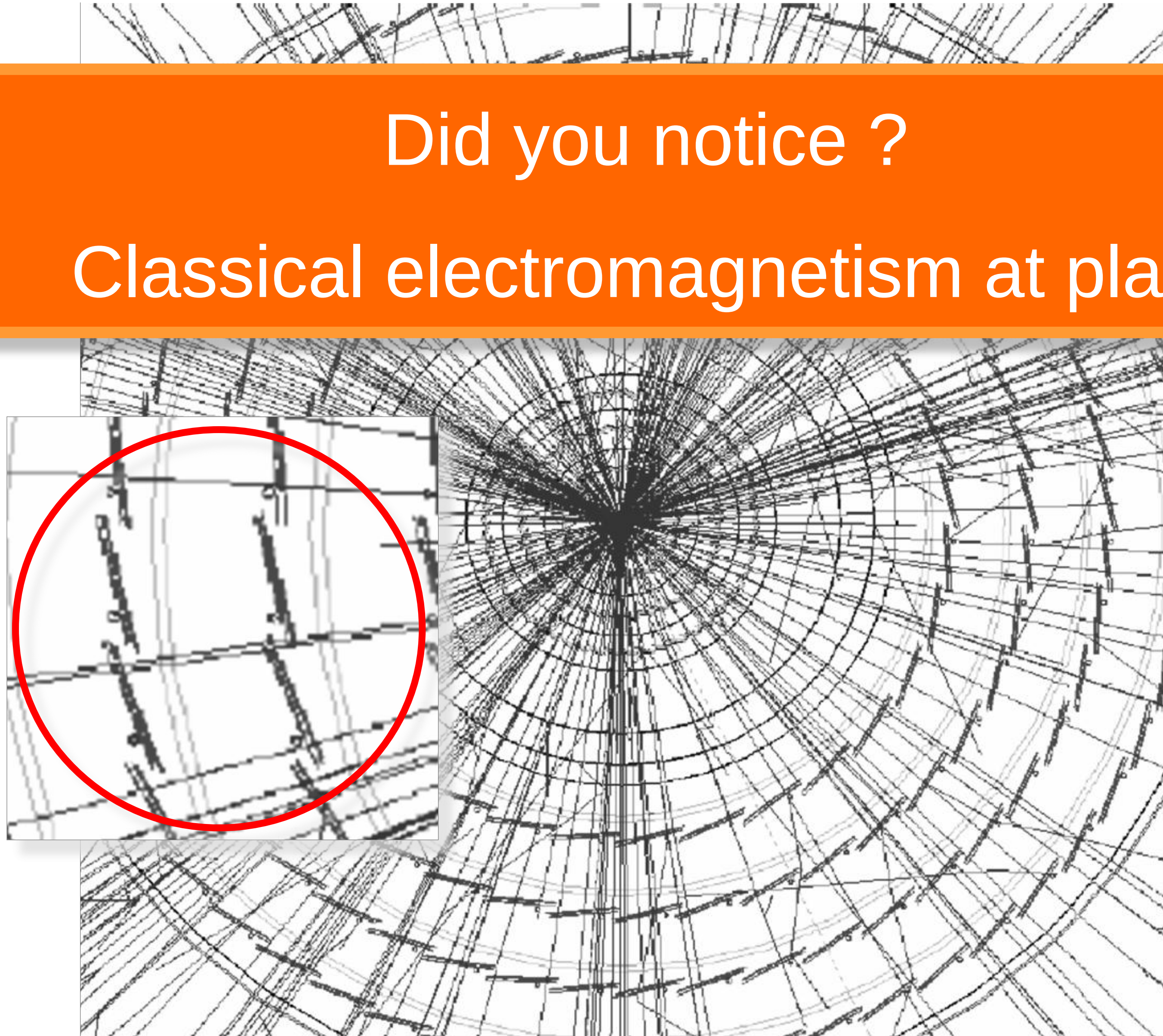

Did you notice ?

Classical electromagnetism at play!

Lorentz Angle Measurement

- The sensors are tilted relative to the pointing axis: SCT (11°) and Pixel (-20°) (*)
  - The charges travelling through the Si substrate are deviated by 2T *B* field (Hall effect)

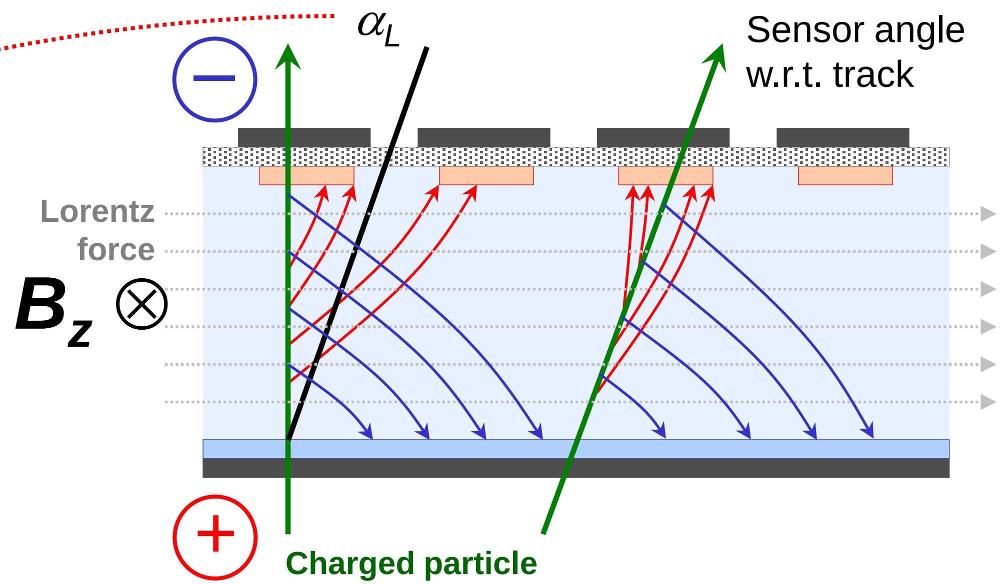

- Lorentz angle determined empirically in test beam by minimising cluster size
- $\alpha_L = f(V_{depl})$ → as bias voltage increases to cope with irradiation, α_L decreaes

(*) The actual Pixel and SCT Lorentz angles are 4° and 12° (no irradiation), and with opposite signs. The tilts chosen are due to technical reasons.

Vertexing and *b*-jet tagging

- The innermost silicon detector must provide the required *b*-tagging efficiency

Good vertex resolution is achieved by placing the **innermost (*B*) layer close to the beam pipe**, and **the next layer farer to it** (lever arm), and by an excellent *B*-layer resolution

Small multiple scattering term: $\sigma_{MS} \sim \frac{1}{p}\sqrt{X/X_0}$

Expected transverse IP resolution ~13 μm for 100 GeV track

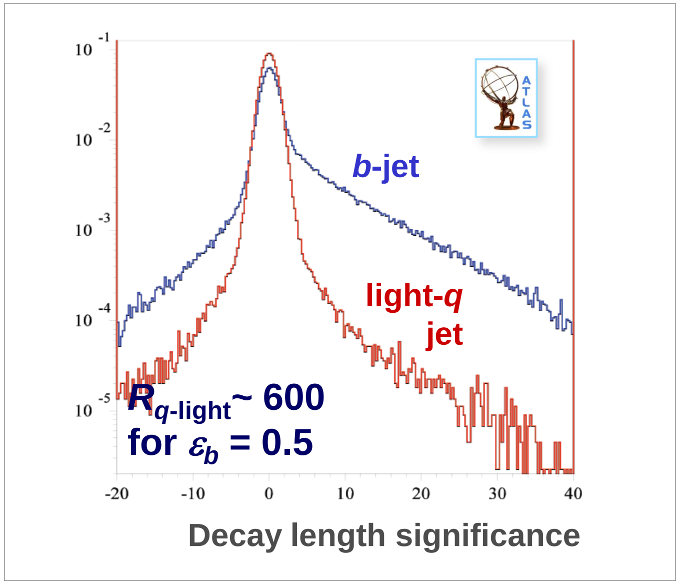

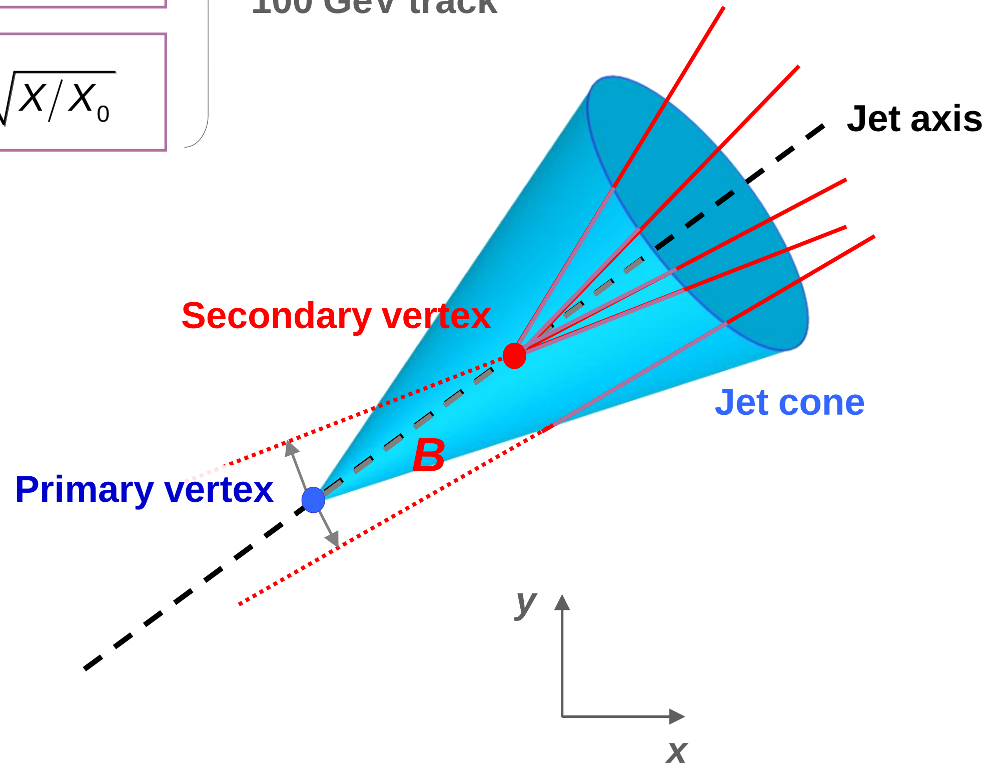

The ATLAS Pixel Detector

- Close to the beam pipe, high track rate invalidates the use of silicon strips
  - Density of tracks in core of jets very high → **true 3D device required → Pixels**
  - Also: leakage currents due to radiation dose require small Si volumes per channel

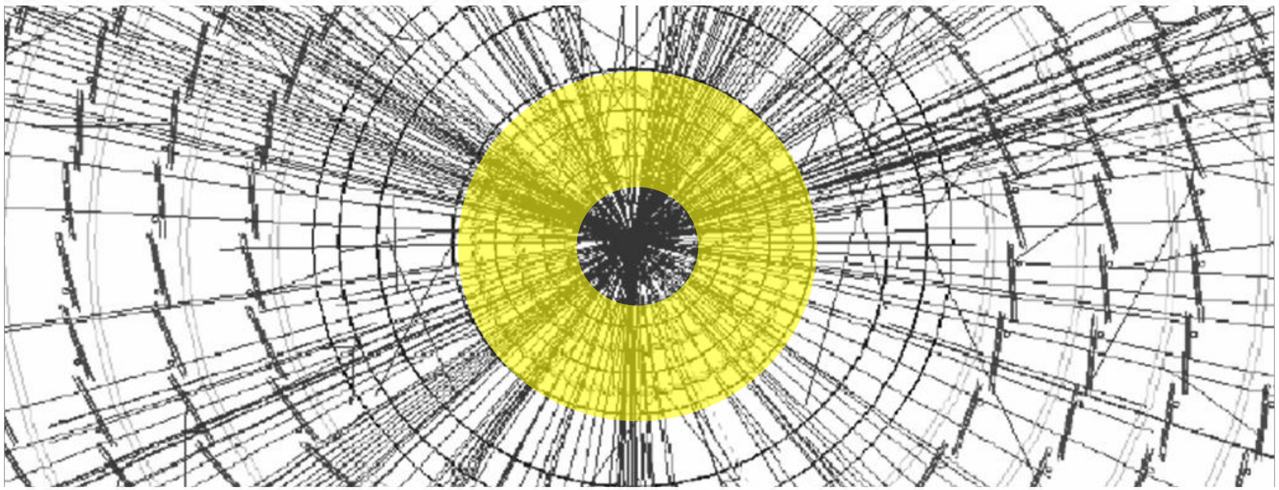

- The ATLAS/CMS pixel detectors are the first generation of high-rate pixel devices
- The basic unit is a **module** (~ 46000 channels)

$pp \to t\bar{t}H(\to b\bar{b})$: ~1200 tracks

The Pixel Module

To cope with high rates, each pixel is read out as an individual electronic channel

Module size: 6×2 cm, 46k pixels: 50[ϕ] × 400[*z*] μm² (250 μm Si bulk), max. bias voltage: 600V, T ≈ –(5–10)°

- 16 front-end chips, each containing 2880 pixel channels with programmable thresholds
- Number of channels: 67×10^6 (barrel) and 13×10^6 (endcap), signal-to-noise > 30
- Zero-suppressed detector read-out: 160 GB/sec
- Area covered by electronics exceeds sensor size
- 6 kW consumption in small active volume requires powerful cooling (evaporative C_3F_8)

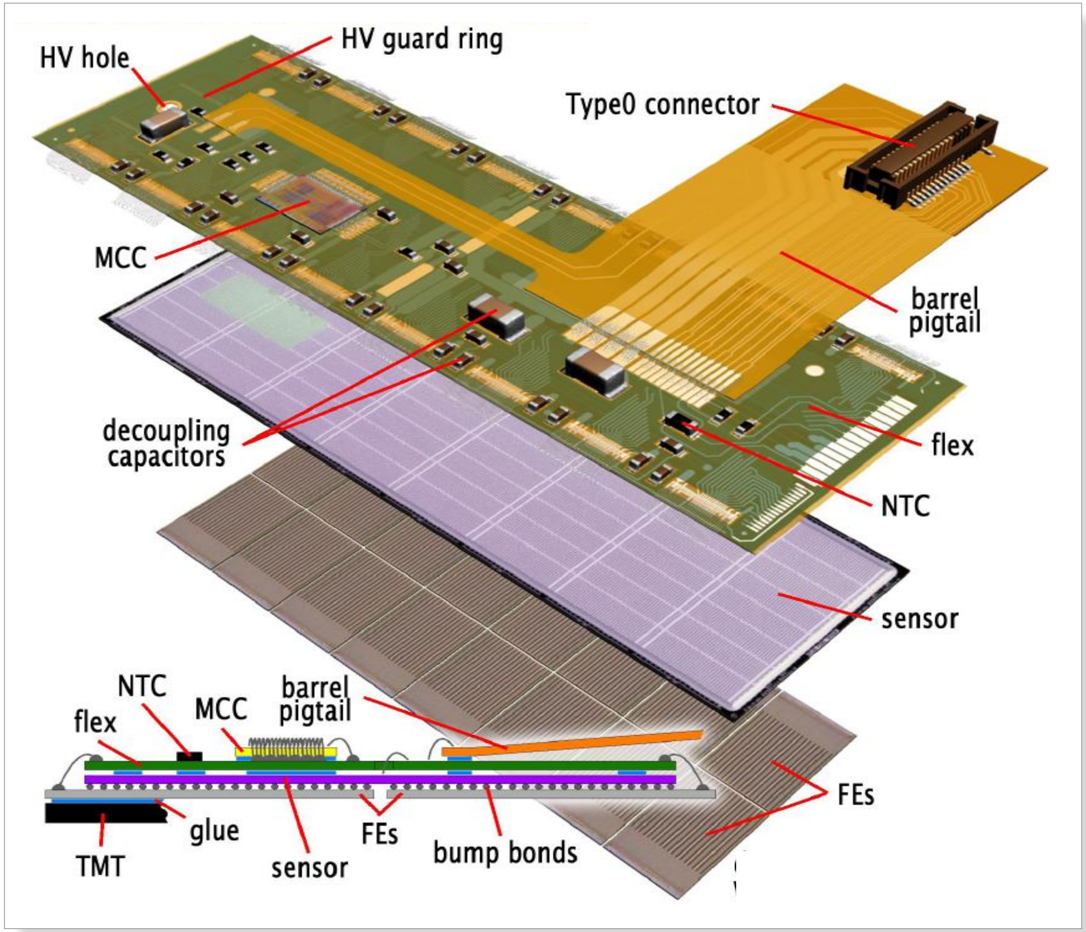

Pixel Sensors in Radiation Environment

- Non-ionising energy loss (NIEL) from irradiation causes irreversible Si lattice damage
  - Increase of leakage current (linear), effective *p* doping, trapping of signal charge
  - "Type inversion" of the bulk

Change of depletion voltage with particle fluence

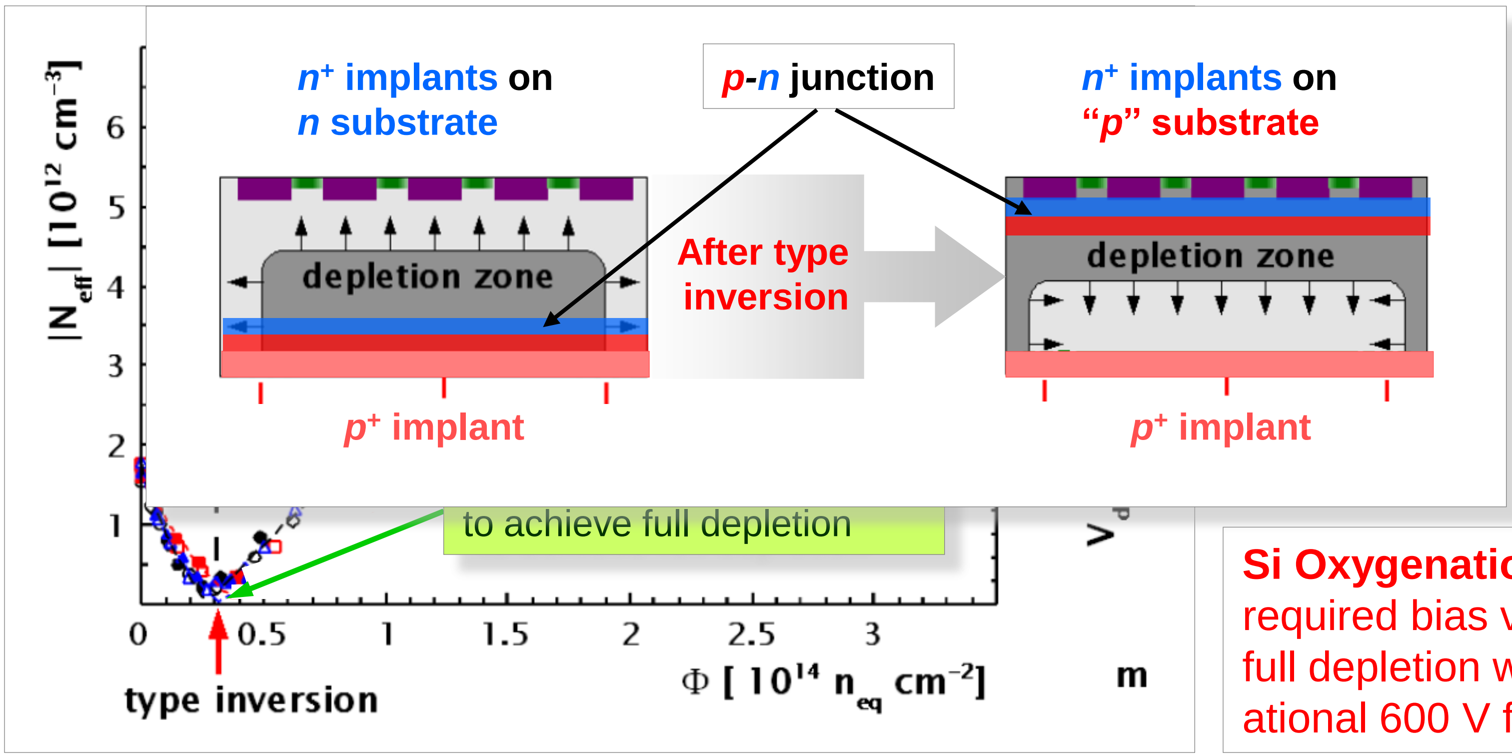

Si Oxygenation: keeps required bias voltage for full depletion within operational 600 V for ~10 yrs

The ATLAS Pixel Detector

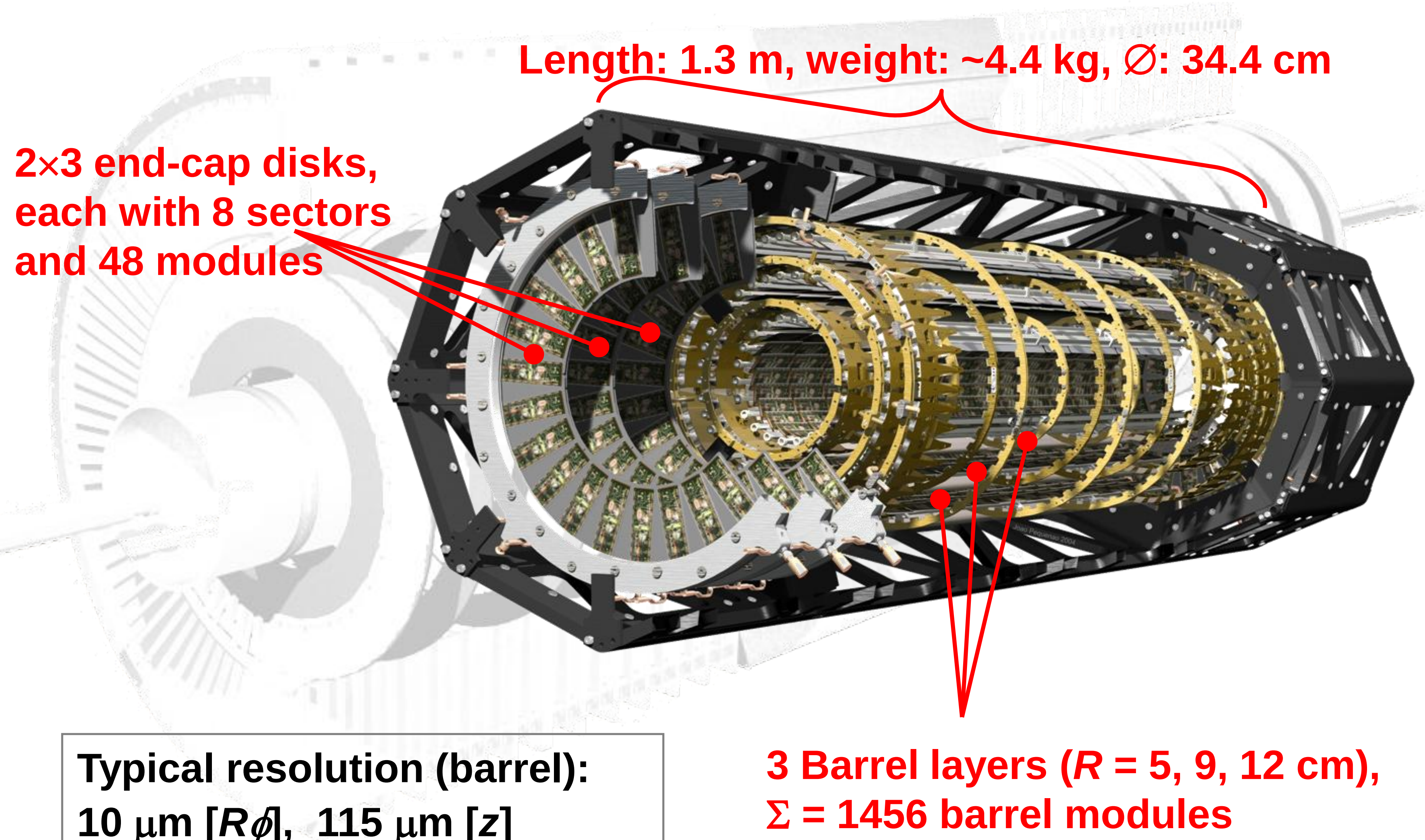

Typical resolution (barrel):
10 μm [*Rϕ*], 115 μm [*z*]

Pixel Pic's

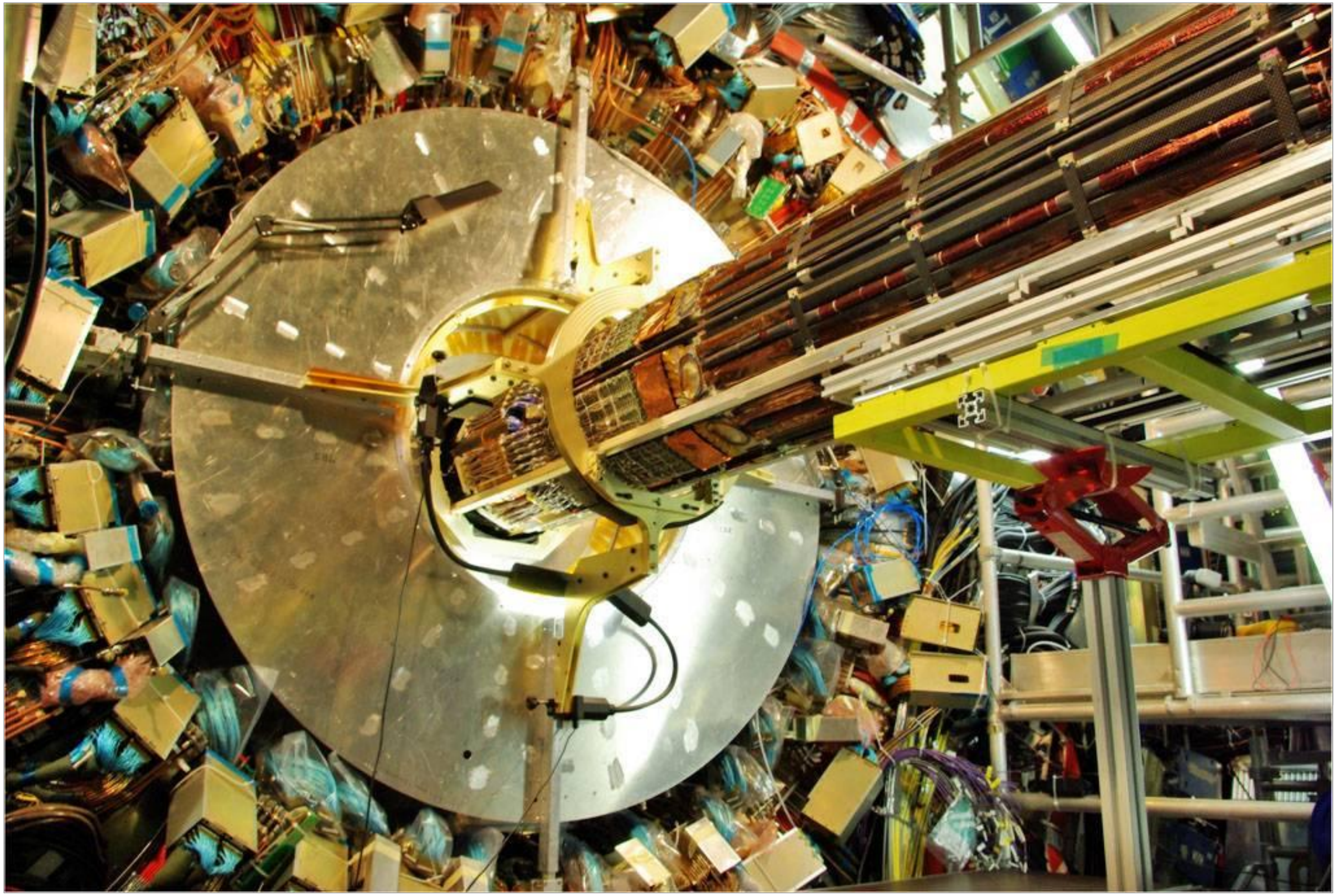

Drift Tubes (DT) in ATLAS: inner detector and muon spectrometer

- Classical detection technique for charged particles based on gas ionisation and drift time measurement

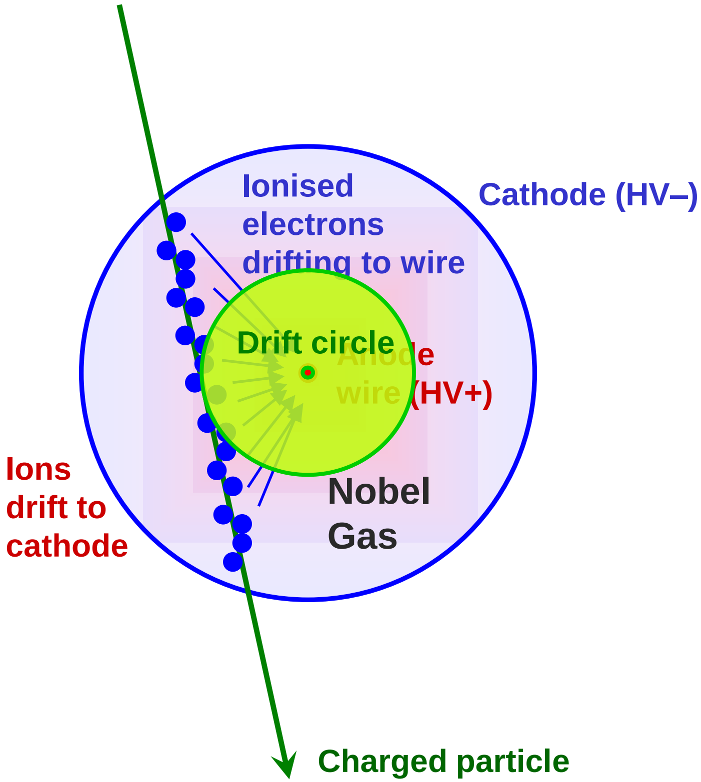

Example: muon in MDTs **(aligned !)**

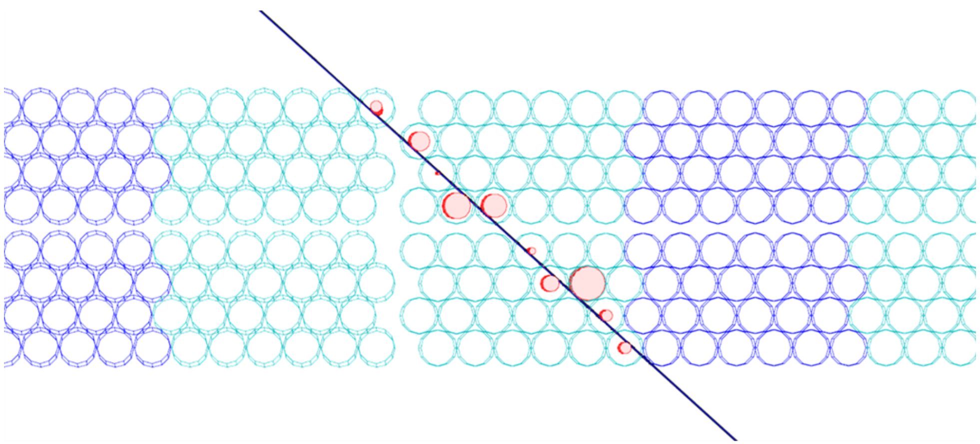

TRT: Kapton tubes, ∅ = 4 mm
MDT: Aluminium tubes, ∅ = 30 mm

Combining Tracking with PID: the ATLAS TRT

- *e*/π separation via transition radiation: polymer (PP) fibres/foils interleaved with DTs

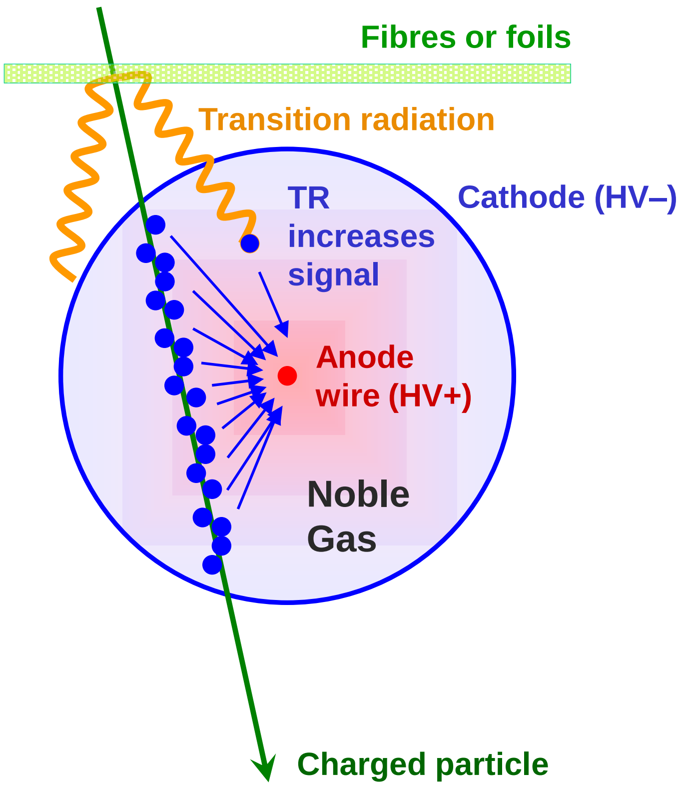

Electrons radiate → higher signal
PID info by counting high-threshold hits

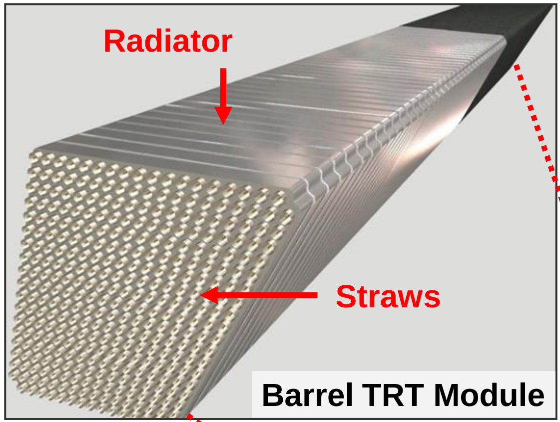

Total: 370k straws

Barrel (|η| < 0.7): 36 r-ϕ measurements / track
Resolution ~130 μm / straw

18 end-cap wheels (|η| < 2.5): 40 or less z-ϕ points

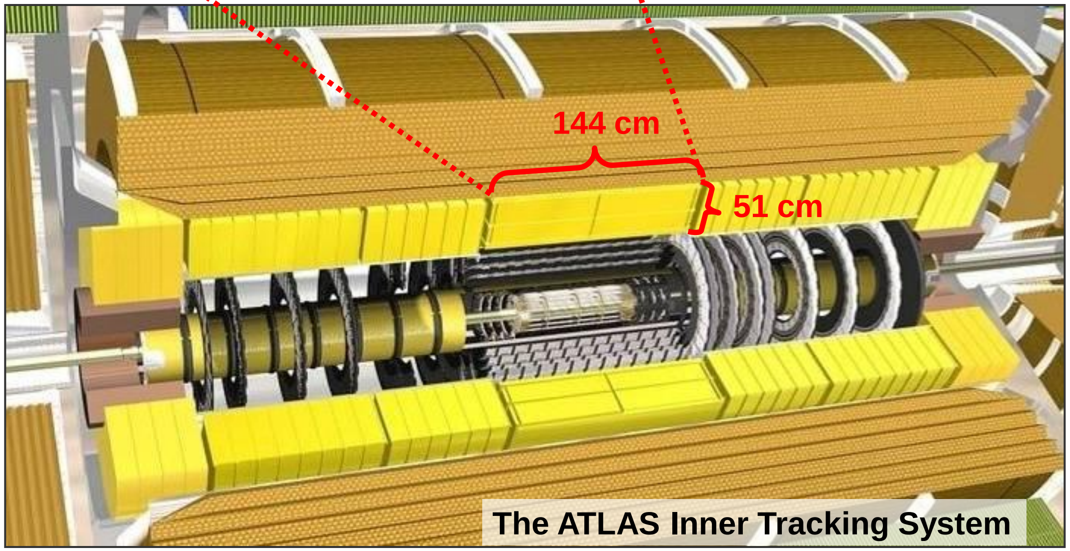

Insertion of SCT into TRT Barrel

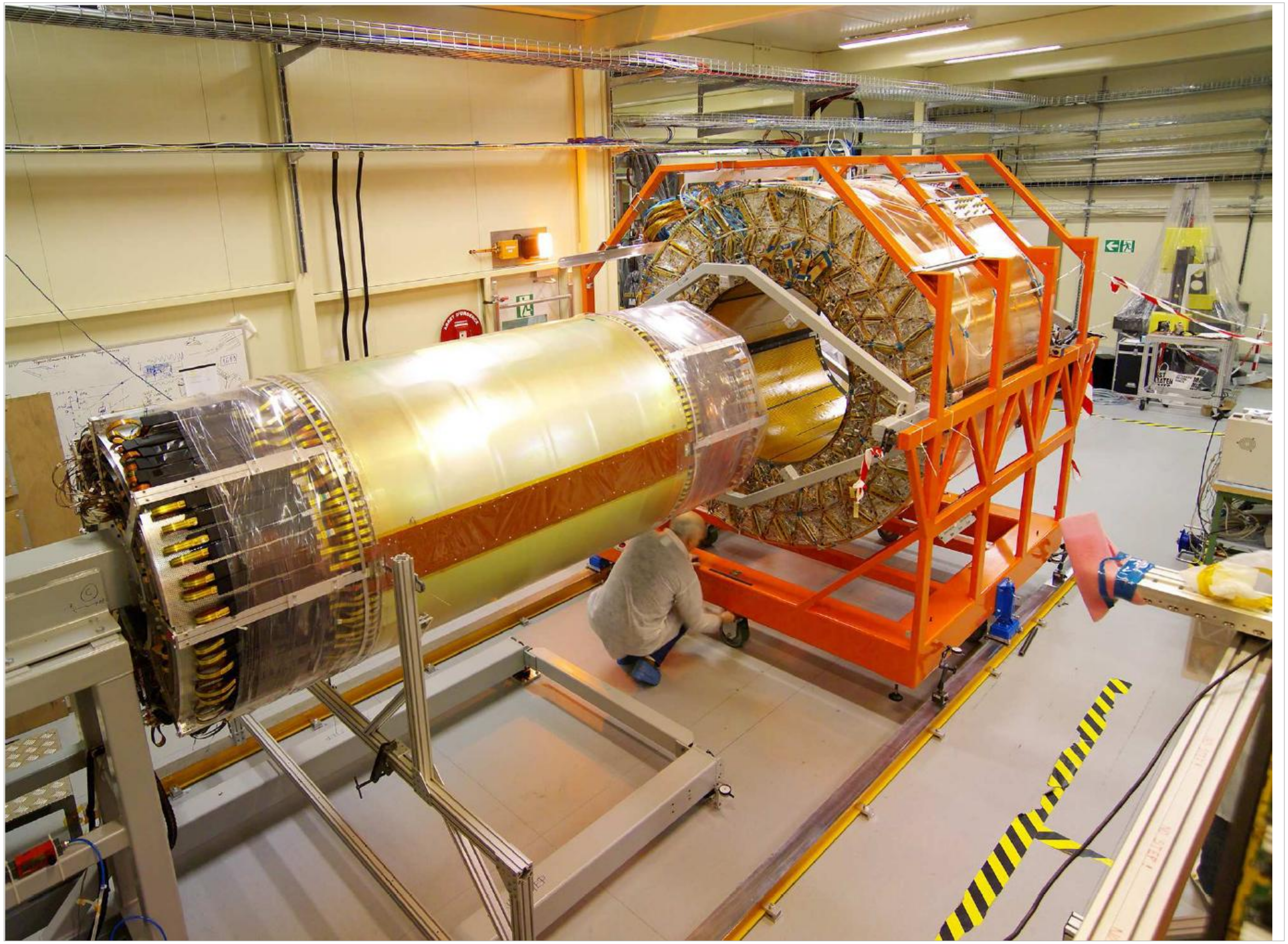

Interlude

Momentum Measurement

Momentum Measurement in Tracking Device

- Charged particles deflection in magnetic field:
  - Lorentz force ⊥ to *B*-field and to particle direction
  - Particle trajectory projected onto plane ⊥ to *B*-field is *circle* with radius: $r\,[\mathrm{m}] = \dfrac{p_T\,[\mathrm{GeV}]}{0.3 \cdot B\,[\mathrm{T}]}$
  - ➧ For p_T = 10 … 1000 GeV and B = 2 T → R = 17 … 1700 m (*cf*, R_{ID} ~ 1 m)
  - ➧ … and if p_T < 0.5 GeV, the particle is trapped in solenoi
- Obtain r and p_T from measurement of sagitta:

$$r \approx \frac{L}{8s} \quad (\text{if } s \ll L) \quad \Rightarrow \quad p_T \propto \frac{1}{s} \quad \text{and} \quad \frac{\sigma(p_T)}{p_T} \propto p_T$$

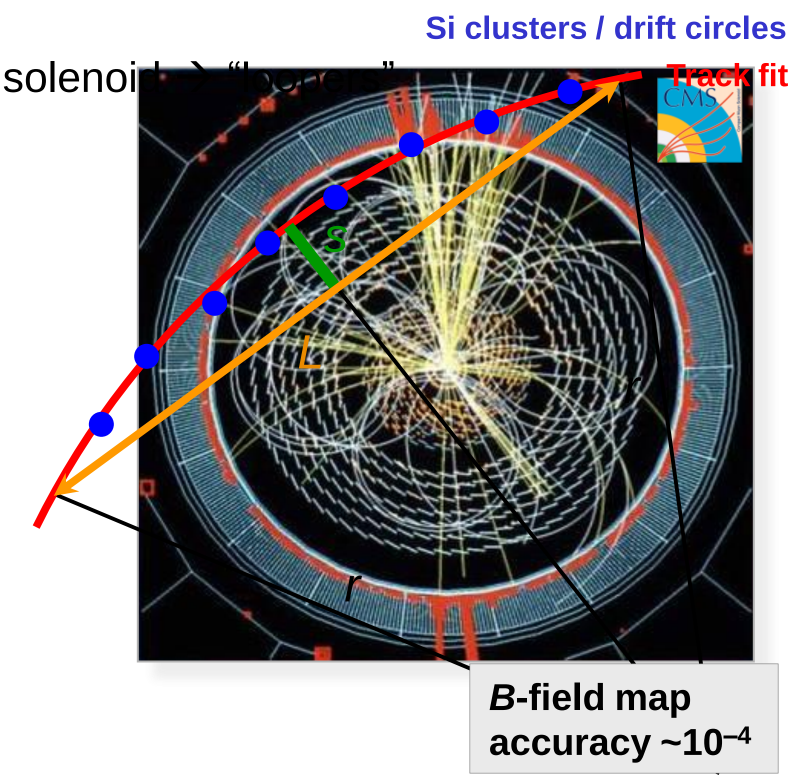

- Track fitting in LHC environment challenging
  - Must handle ambiguities, hit overlaps, multiple scattering, bremsstrahlung, multiple vertices, …
  - Track fitters take Gaussian noise (Kalman) and non-Gaussian noise (GSF) into account
  - Fitter must be fast, used in high-level trigger

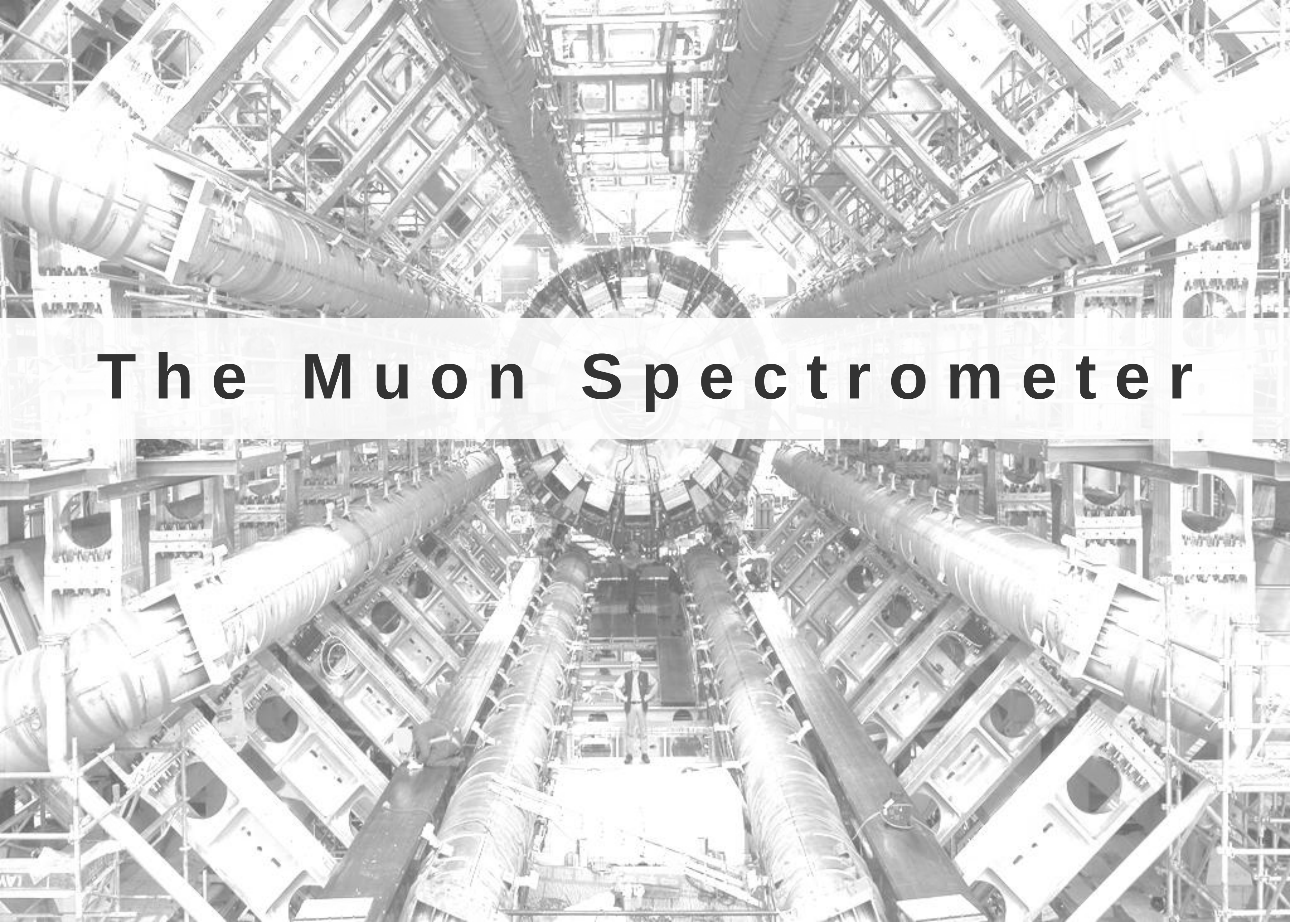

The Muon Spectrometer

The ATLAS Muon Spectrometer (Active Material)

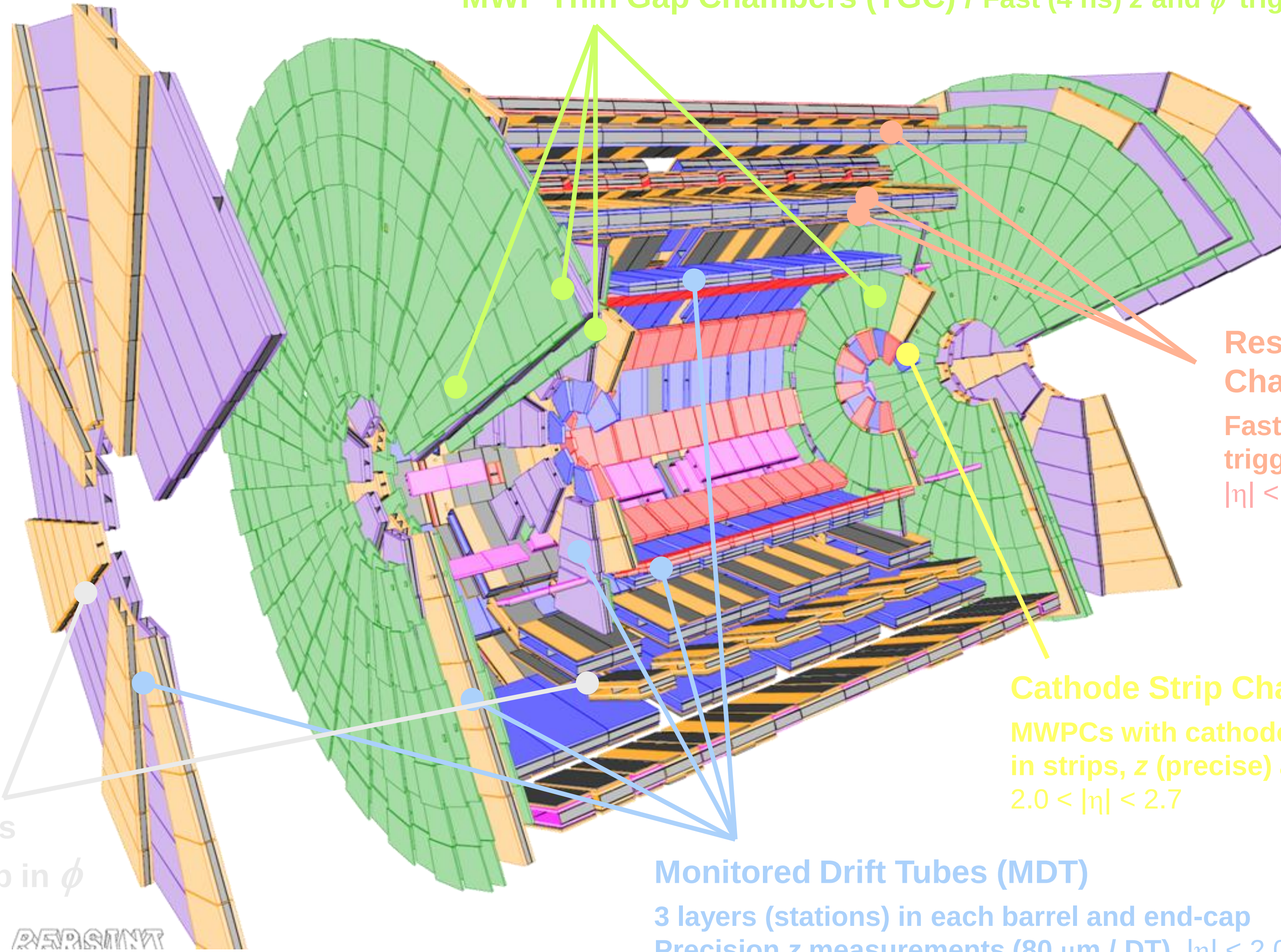

The ATLAS Muon Spectrometer

- Outer layer of LHC detectors, only reached by WI(M)Ps (ν, χ) or EM MIPs (μ)
  - Good containment of jets requires ~11 λ before muon systems
  - ATLAS opted for good stand-alone tracking if too high-backgrounds in ID
- Huge magnetic volume
  - ATLAS has 8 (barrel) 3 T_{max} and 2×8 (endcap) 6 T_{max} superconducting toroid magnets

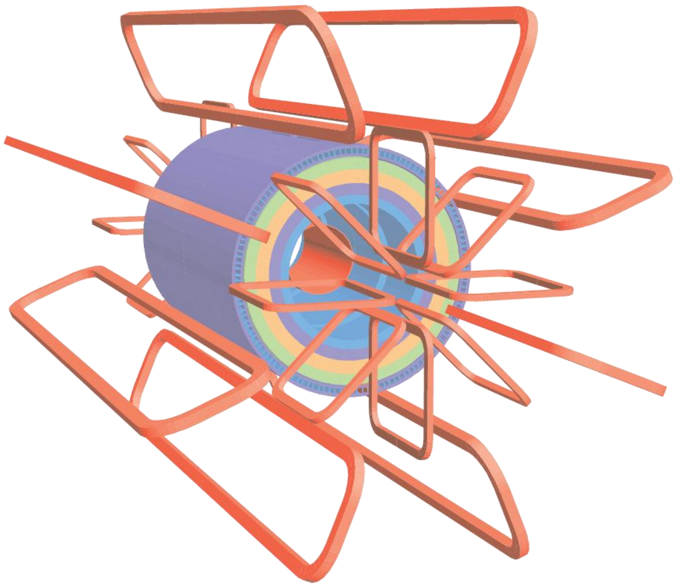

- Huge active detectors area
  - Open structure minimises multiple scattering
  - Dedicated trigger chambers
- Huge mechanical structure
  - Challenging tolerances for mechanical stability, positioning and alignment (optical sensors)

ATLAS Toroid Fields

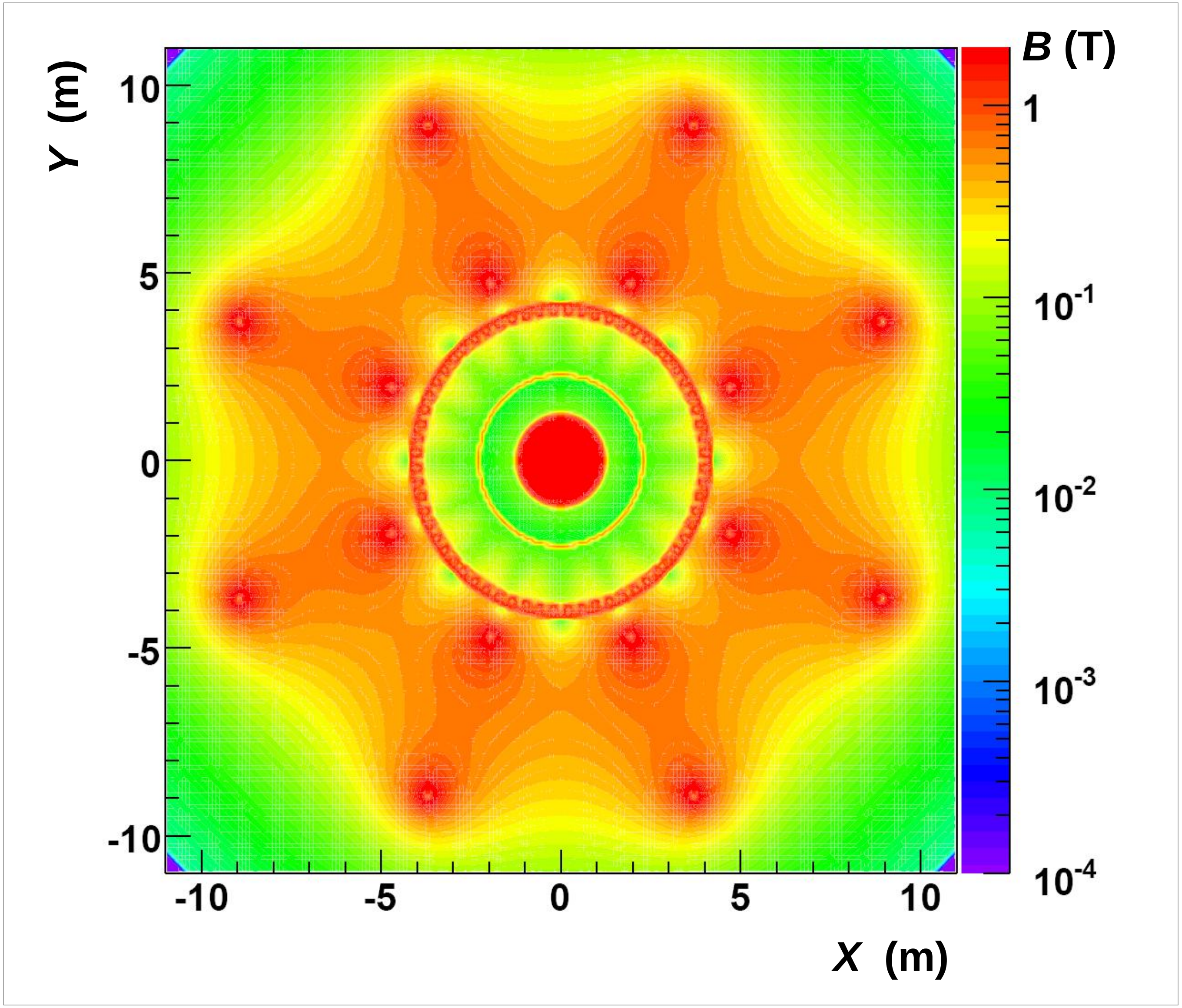

Momentum Measurement

- Toroid fields bend tracks in ***z* direction**, instead of *R* -ϕ as in the inner detector

  $\sigma(z)$ = 35 μm per chamber → $\sigma(s) \approx (3/2)^{1/2} \cdot \sigma(z)$ = 43 μm

  → 1 TeV track has *s* = 500 μm at $\eta \approx 0$ → < 10 % precision on momentum measurement

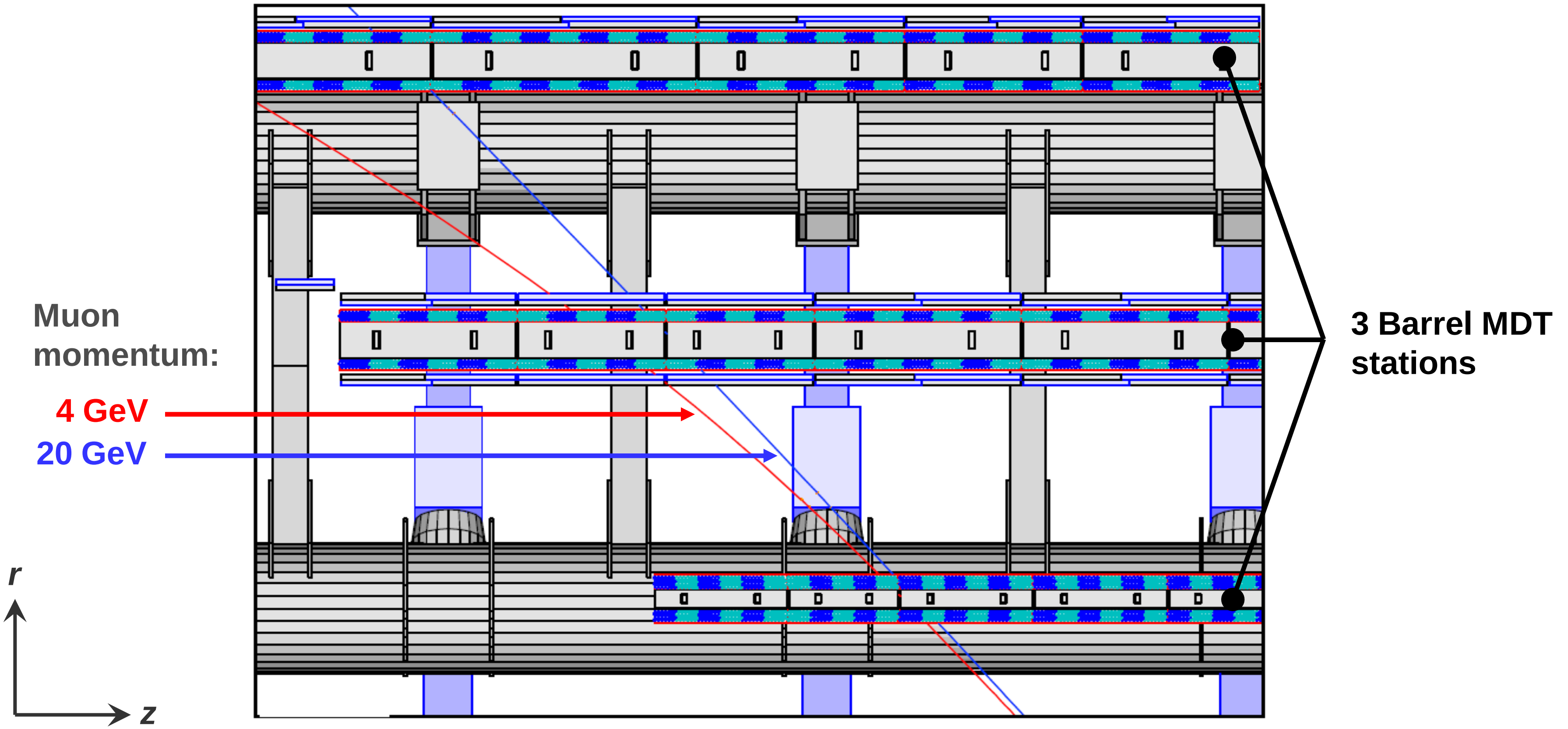

Triggering Muons

- Ultra-fast L1 trigger requires coincident hits in 3 RPC (barrel) or 3 TGC (end-caps) layers within “roads” corresponding to predefined momenta (thresholds)

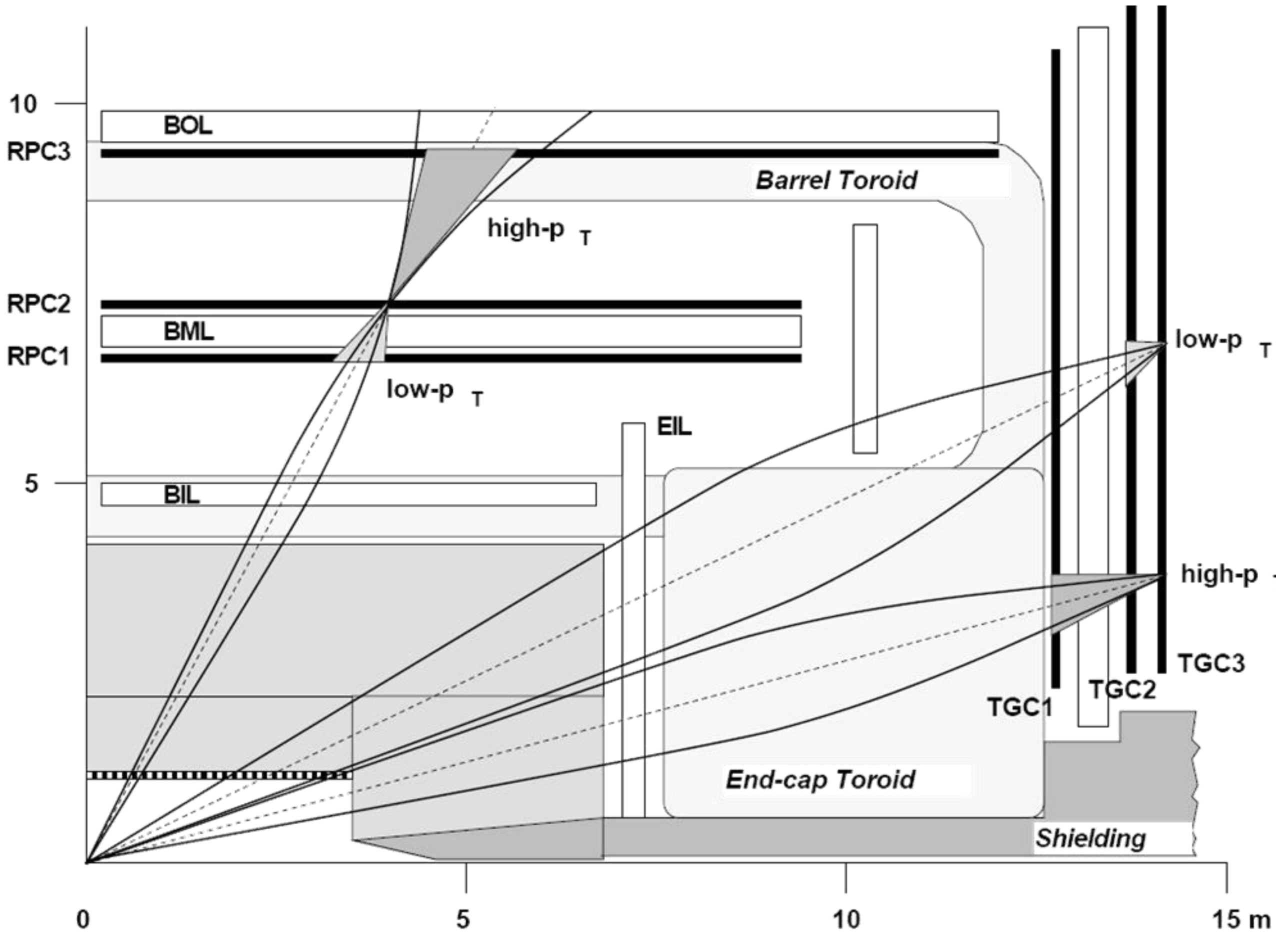

The ATLAS Muon Spectrometer

Big wheel, Feb 2007